University of Nevada, Reno

Modeling Oxytocin-Induced Neurorobotic Trust and Intent Recognition in Human-Robot Interaction

A thesis submitted in partial fulfillment of the
requirements for the degree of Master of Science in
Computer Science

by

Sridhar Reddy Anumandla

Dr. Sergiu Dascalu, Thesis Advisor

Dr. Philip H. Goodman, Thesis Co-advisor

December 2010

University of Nevada, Reno
Statewide • Worldwide

THE GRADUATE SCHOOL

We recommend that the thesis
prepared under our supervision by

SRIDHAR REDDY ANUMANDLA

entitled

Modeling Oxytocin-Induced Neurorobotic Trust and Intent Recognition in Human-Robot Interaction

be accepted in partial fulfillment of the
requirements for the degree of

MASTER OF SCIENCE

Sergiu Dascalu, Ph.D., Advisor

Philip H. Goodman, M.D., M.S., Co-advisor

Frederick C. Harris, Jr., Ph.D., Committee Member

Monica Nicolescu, Ph.D., Committee Member

Jordan T. Hastings, Ph.D., Committee Member

Pavel Solin, Ph.D., Graduate School Representative

Marsha H. Read, Ph.D., Associate Dean, Graduate School

December 2010

Abstract

Recent human pharmacological fMRI studies suggest that oxytocin is a centrally-acting neurotransmitter important in the development and expression of trusting relationships in men and women, distinct from its role as a peripheral hormone related to parturition and lactation. Oxytocin administration in humans increases trust, acceptance of social risk, memory of faces, and inference of the emotional state of others, at least in part by direct inhibition of the amygdala. The cerebral microcircuitry underlying this mechanism remains unknown. Here, we propose a spiking integrate-and-fire neuronal model of several key interacting brain regions affected by oxytocin neurophysiology during social trust behavior. Because modeling social interactions requires near real-time responsiveness, we embodied the brain simulator in a behaving virtual humanoid neurorobot which “sees” a human by way of a camera system designed to capture motion of edges in the environment. Tonic firing of the amygdala is modeled using the recurrent asynchronous irregular nonlinear network architecture. Oxytocin cells are modeled with triple apical dendrites characteristic of their structure in the paraventricular nucleus of the hypothalamus. We demonstrate the success of this hybrid system in learning trust by discriminating between concordant versus discordant movements of a human actor, which leads to cooperative versus protective behavior by the neurorobot when challenged by a new intent from the human. Implications for further research and future design of socially intelligent neurorobotic systems are also presented.

Dedication

I would like to dedicate this work to Dr. Philip Goodman who had always been a great mentor and a role model without whom this work would have been incomplete, and to my parents Soma Reddy and Poolamma who have been supporting me strongly in shaping up my career and always strived for my success; without them I would have been nowhere. I owe them eternal respect and unbounded gratitude.

Acknowledgements

I would like to thank Dr. Philip Goodman for providing me a wonderful opportunity to work on this project and be a part of the Brain Computation Lab. I would also like to express my deepest thanks to him for his invaluable guidance and encouragement throughout this project.

My sincere thanks to Dr. Sergiu Dascalu for serving as my thesis committee chair, devoting his precious time for suggestions and guiding me in the right direction. He has always been a great mentor and a motivating person. I am grateful to Dr. Frederick Harris and Dr. Jordan Hastings for serving on my thesis committee, and for supporting me throughout the graduate school. I am also grateful to Dr. Monica Nicolescu and Dr. Pavel Solin for being part of my thesis committee and providing valuable feedback on my thesis.

Furthermore, I am very thankful to Corey Thibeault for providing me invaluable insight into the work at the Brain Computation Lab, and for his cooperation and assistance during the course of this project. Many thanks go as well to Laurence Jayet Bray for assisting me to understand biological concepts.

I would also like to thank the Office of Naval Research and DARPA-HRL for providing financial support for this project.

Finally, it is a pleasure to thank my brother and sister Srikanth and Shalini, and my friends Bharathi and Rajeev for their love and support during every hardship.

Table of Contents

List of Figures

List of Tables

List of Acronyms

AI	Artificial Intelligence
ANN	Artificial Neural Network
AP	Action Potential
CNS	Central Nervous System
CPU	Central Processing Unit
DOF	Degrees Of Freedom
EA	Evolutionary Algorithms
FL	Fuzzy Logic
FOV	Field Of View
GENESIS	General Neural Simulation System
GPU	Graphics Processing Unit
GUI	Graphical User Interface
ITI	Instinctual Trust the Intent
LSD	Long-term Synaptic Dynamics
MPI	Message Passing Interface
NCS	NeoCortical Simulator
NEST	Neural Simulation Tool
NN	Neural Networks
ODE	Open Dynamics Engine
OT	Oxytocin
PVN	Paraventricular Nucleus
RAIN	Recurrent Asynchronous Irregular Nonlinear
SON	Supraoptic Nucleus
SSD	Short-term Synaptic Dynamics
URBI	Universal Real-Time Behavior Interface
USE	Utilization of Synaptic Efficacy
VHNR	Virtual Humanoid Neurorobot
VNR	Virtual Neurorobotics
VRML	Virtual Reality Modeling Language

Chapter 1: Introduction

There are many mysteries involved in the functioning of a mammalian brain. It is considered as a complex network of interconnected neurons. There has been a lot of research in understanding the theory behind memory, consciousness, and behavior. The fundamental activity observed in a mammalian brain is that it receives information from the sensory organs through vision, auditory, tactile, smell, and taste, and these stimuli are responsible for neuronal activation and transmission of activity to interconnected neurons in the network via synapses. This activity results in stimulating a specific region of the brain whose role might be to perform a motor action corresponding to the region.

The field that deals with the design of intelligent agents using computational and mathematical techniques is called Artificial Intelligence (AI). An intelligent agent makes decisions based on the information it perceives from the environment that maximizes its chances of precise completion of tasks. After considerable research people started realizing that there are many limitations in AI and it is not possible to create an intelligent machine that closely mimics a human.

An alternative approach to AI is computational neuroscience that deals with modeling biological elements of a nervous system based on the parameters collected from *in vivo* and *in vitro* experiments. The simulation of biological nervous system is performed with the help of neural simulation software running on a cluster in order to produce biologically realistic spiking neural network simulations. NEURON [24], General Neural Simulation System (GENESIS) [24], and Neural Simulation Tool (NEST) [24] were the first simulation software packages introduced into market, which are capable of simulating individual neurons and small scale realistic networks of neurons. In order to model large scale biologically realistic networks, a simulation software called NeoCortical Simulator (NCS) [24] was developed by the Brain Computation Lab at the University of Nevada, Reno under the guidance of Dr. Philip Goodman. NCS is capable of modeling thousands of cells and millions of neurons, and is flexible enough to accommodate vision and auditory systems.

The research presented in this thesis provides an insight into several functions performed by the oxytocin (OT) on various parts of a human body starting from well-

known reproductory functions in females to recently explored higher cognitive functions such as trust, social bonding, and suppression of fear in mammals. The goal of the work presented in this thesis has been to explore the neural mechanism related to the establishment of trust from published *in vivo* experiments, model it using the NCS, and implement it on a virtual robot in order to emulate the behavior of a mammalian brain. Additionally, we sought to develop a biologically realistic neuromorphic brain such that the parameters and mechanisms to be used should be close to published *in vivo* recordings.

Our contributions to the study presented in this thesis are modeling the cortical columns and limbic systems of a mammalian brain, developing the robotic interface to implement the experiment's human-robot interaction, integrating various components of the experiment to demonstrate the Instinctual Trust the Intent (ITI) scenario, and making the model more biologically realistic by introducing the existing triple apical dendrite model within the hypothalamus and the Recurrent Asynchronous Irregular Nonlinear (RAIN) activity in the amygdala.

The rest of this thesis is organized as follows. In Chapter 2, the basic elements that constitute a brain, effects of OT on female reproductory system and various parts of a mammalian brain, cortical columns and their functions, and brainstem are discussed. In general, this chapter provides an overview of the biological concepts that are essential to understand the work presented in this thesis. Chapter 3 reviews several popular brain simulators that are currently being used in the market, provides a brief description of robotics, and introduces the webots simulation package that was used to design the virtual humanoid neurorobot and program the controller for the experiment presented in this thesis. This chapter provides a technical background for the work presented in this thesis. Chapter 4 provides a detailed description about the instinctual trust the intent scenario, individual components of the experiment, and the computational brain model developed to simulate trust. Chapter 5 discusses results of the study. Finally, the conclusions and possible scope of future work are discussed in Chapter 6.

Chapter 2: Biological Background

In any living organism the brain can be considered a kind of Central Processing Unit (CPU) with enormous processing power. It is composed of certain well-known fundamental biological entities and mechanisms that play a prominent role in accumulating information from the sensory inputs, neural transmission of processed information, and electrical stimulations of different regions in the brain analogous to the type and intensity of sensory stimuli. The NCS was developed based on these fundamental biological concepts and incorporates complex models to unveil the secrets of functions performed by the brain. This chapter provides an introduction to the fundamental biology of a mammalian brain in view of building complex brain models, offers insights into the regions of the brain that are involved in the establishment of trust and suppression of fear, describes the sensory-association-motor cortical columns, and the brainstem.

2.1. Overview of Biological Concepts

A mammalian brain consists of many complex structures of which the neocortex is of special focus to us since it plays a key role in sensory perception, spatial navigation, memory, attention, and cognition [30, 35]. The neocortex is divided into four different regions called frontal, parietal, occipital, and temporal lobes; each of them is defined to perform a specific function. For example, the frontal lobe is associated with memory and attention apart from other casual functions, the parietal lobe is associated with integrating sensory information and results in spatial navigation, the occipital lobe is associated with visual processing, and the temporal lobe is associated with auditory processing. The four regions of the neocortex are illustrated in Figure 2.1.

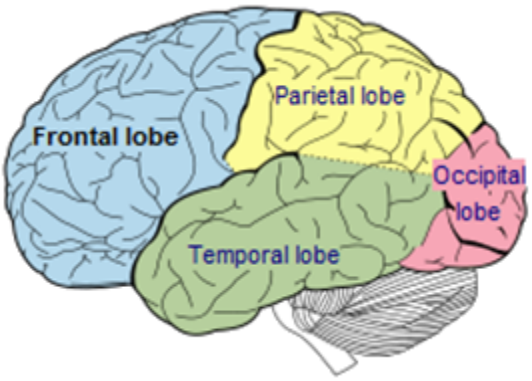

Figure 2.1 The lobes of the brain [6]

Neurons

The neuron is the basic component of the brain that processes and transmits information in the form of electrical and chemical signals. A neuron is a particular type of cell that is excited by electrical stimulations from other cells. A mammalian brain is very complex and according to Sapp (1999) [70], an adult human brain contains more than 100 billion neurons. Connections between these neurons result in highly complex and intelligent Neural Networks (NN). There are three different classes of specialized neurons present in the brain [8]: afferent neurons that receive excitatory sensory stimuli from sensory organs and transmit them to Central Nervous System (CNS); efferent neurons that receive stimuli from CNS and transmit them to effector cells such as the motor neurons that receive signals from the brain to perform different muscle movements; and interneurons [36], which have connections between neurons of the same region. The structure of a typical neuron is shown in Figure 2.2.

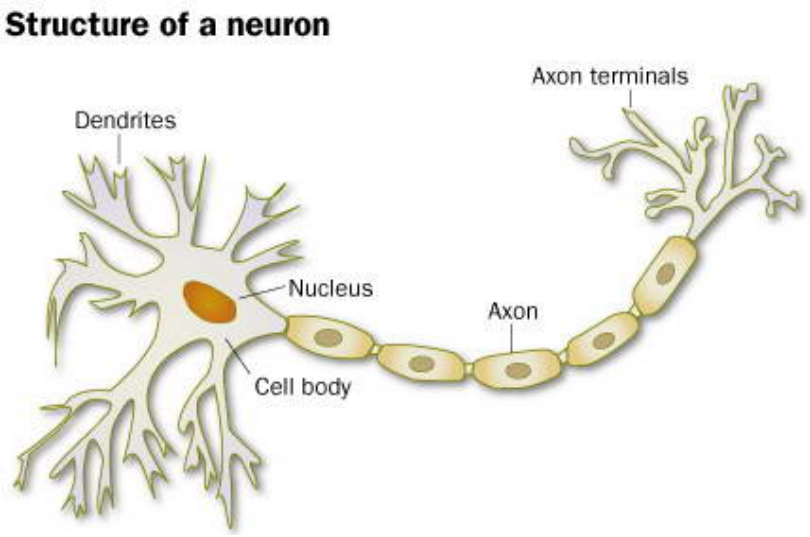

Figure 2.2 A neuron [10]

A typical neuron consists of a cell body called soma with a nucleus and many terminals called dendrites extending from the soma. The dendrites are responsible for receiving stimuli from neighboring excitable cells that have reached their threshold and cause firing of an Action Potential (AP). This exchange of electrochemical information with other neurons is carried out through synapses (described later in this section). The soma receives input from all the dendrites, aggregates them and fires an AP if the aggregate has reached a threshold. This process of firing an AP is called integrate-and-fire. An axon is a long dendrite covered by a myelin sheath that is responsible for carrying electrochemical signals from the soma to other neurons. The electrochemical information from one neuron is transmitted to another via axon-dendrite terminals with the help of synapses [65].

Action Potential

A neuron receives input from neighboring neurons, fires an AP, and transmits it to other connected neurons respectively. This process occurs when a significant amount of stimuli are received by the brain. Connections between neurons are established with the help of axons, dendrites, and synapses. A complex network of neurons is formed because of these connections. A small electrical potential of about -70mV is maintained in the soma of a neuron because of channels that are present in the cell interacting with ions of

intercellular fluid [65]. This electrical potential changes (raises and falls) rapidly depending on the external stimuli received by the incoming synapses. The stimuli from other neurons are aggregated at the soma and when the resulting voltage reaches a spiking threshold the membrane potential of a cell varies by causing an abrupt rise and fall. This change in voltage causes a spike to fire and is termed AP. Figure 2.3 presents a schematic representation of an AP.

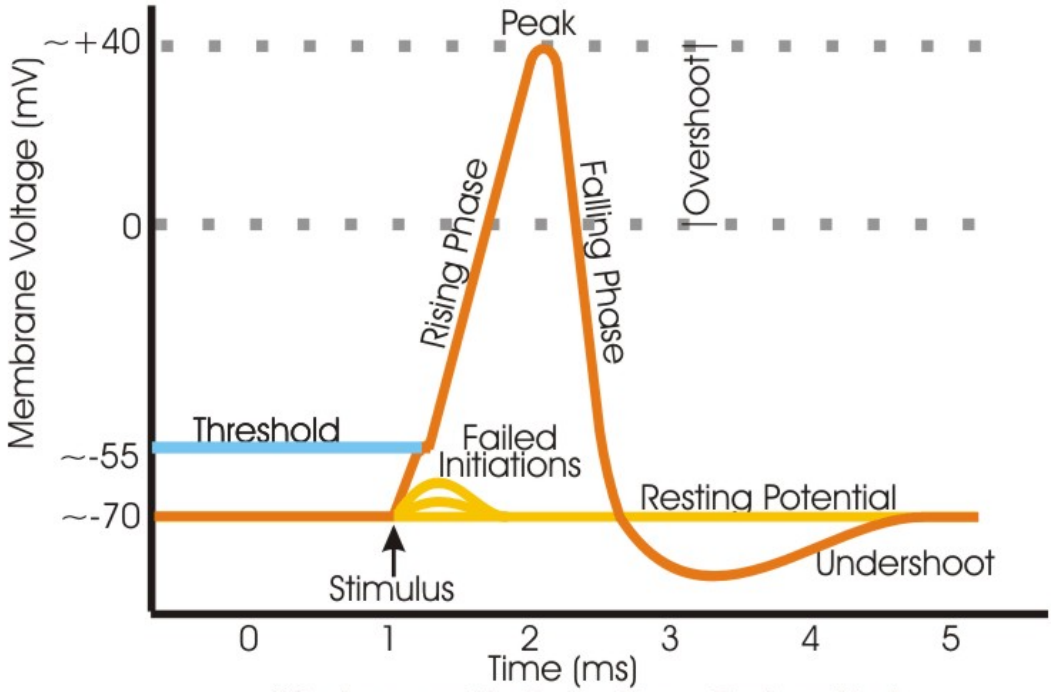

Figure 2.3 Example of AP [1]

Synapse

As we know there are 100 billion neurons in an adult human brain and each of these neurons has on average 7,000 synaptic connections with other neurons. The brain of a three year old child is estimated to have around 10^{15} synapses and the number of synapses decrease with age. An adult brain is estimated to have between 10^{14} and 5×10^{14} synapses [29].

The electrochemical information of a neuron is transmitted to another neuron via a synapse. Figure 2.4 shows the structure of a synapse. Neurons are separated by a small gap present in the synapse. A synapse is primarily composed of three structures:

1. The terminal of an axon (axon ending) of a pre-synaptic neuron, which contains neurotransmitters located inside vesicles, mitochondria, and other cell organelles.
2. A synapse cleft or synaptic gap between pre-synaptic and post-synaptic neurons.
3. A dendrite of a post-synaptic neuron containing receptor sites which are ready to receive the neurotransmitters.

As mentioned above, electrochemical information from one neuron to another is transmitted via a synapse in the form of a spike generated by an AP. A synapse contains a synaptic cleft which is a small gap between the axon terminal of one neuron and the dendrite of another neuron that is filled with extracellular fluid. The neuron at which an AP is generated is called a pre-synaptic neuron (source) and the neuron which receives it is called a post-synaptic neuron (destination). The pre-synaptic and post-synaptic neurons are separated by a synaptic cleft.

When an AP is generated in the pre-synaptic neuron it traverses through the axon and reaches the end of the pre-synaptic neuron. At this time, due to an electrical impulse the migration of vesicles (tiny bubbles) containing neurotransmitters takes place. The vesicles move towards the pre-synaptic membrane where the membrane of vesicles fuses with the membrane of a pre-synaptic neuron and thus releases the neurotransmitters into the synaptic cleft. The neurotransmitters flow across the synaptic cleft and reach the membrane of a post-synaptic neuron that contains receptor sites waiting for the neurotransmitters. Finally, the neurotransmitters are accepted by the receptor sites and this will affect the excitability of a post-synaptic neuron. The spike received by the post-synaptic neuron is integrated with all the other inputs from other neurons and if the resultant value reaches the threshold then a spike is generated in the post-synaptic neuron, and the whole process is repeated.

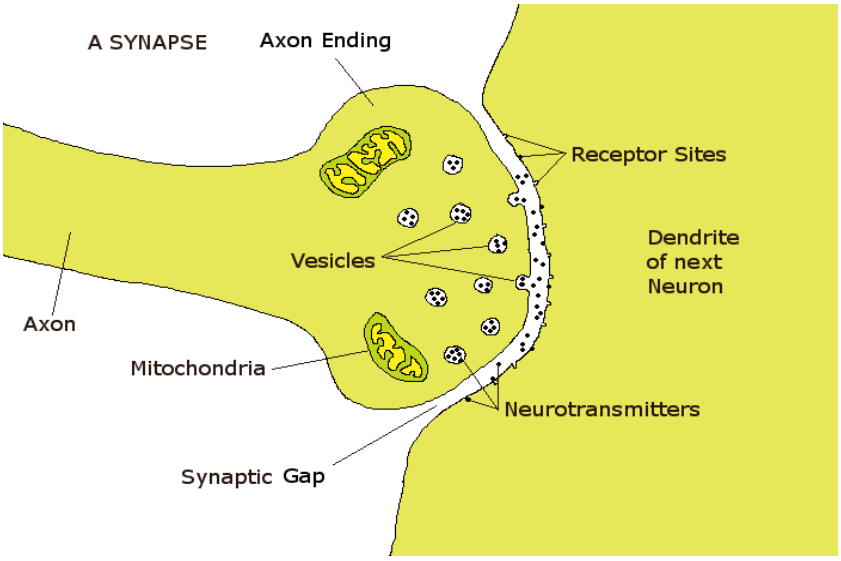

Figure 2.4 A synapse [12]

The synaptic connection between pre-synaptic and post-synaptic neurons can be one of the three types [14], as follows:

1. Axodendritic: The axon of a pre-synaptic neuron connects to the dendrite of a post-synaptic neuron.
2. Axosomatic: The axon of a pre-synaptic neuron connects to the cell body (soma) of a post-synaptic neuron.
3. Axoaxonic: The axon of a pre-synaptic neuron connects to the axon of a post-synaptic neuron.

Figure 2.5 shows the three different types of synaptic connections between two neurons.

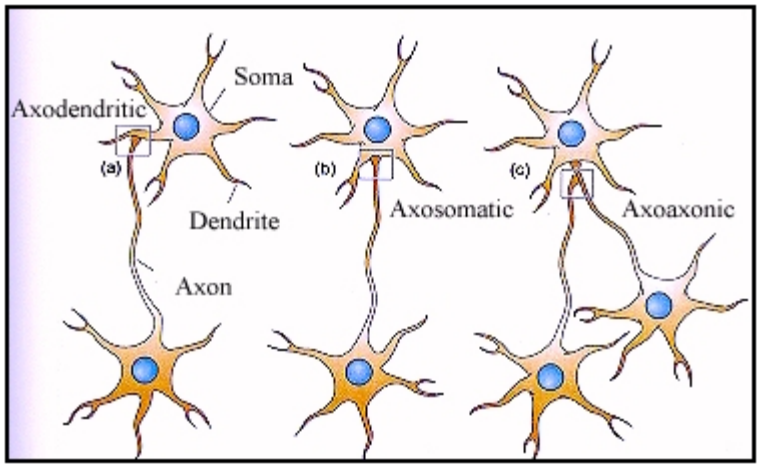

Figure 2.5 Synaptic connections between two neurons [5]

Synapses are of two types: excitatory and inhibitory. An excitatory synapse connecting from the pre-synaptic neuron to the post-synaptic neuron causes the post-synaptic neuron to fire (depolarize) whereas an inhibitory synapse suppresses the firing of the post-synaptic neuron (repolarize). This ability of a synapse to depolarize or repolarize is regulated by Short-term Synaptic Dynamics (SSD) called facilitation and depression, and Long-term Synaptic Dynamics (LSD) called Hebbian learning [73]. Based on whether a synapse depolarizes or repolarizes its Utilization of Synaptic Efficacy (USE) is affected. This effect could result in either release of more neurotransmitters (boosting up the signal) or less neurotransmitters (diminishing the signal).

The SSD controls the release of neurotransmitters within a specified window interval. The USE value is affected by the facilitation and depression time constants. The facilitation time constant increases the effectiveness of a synapse whereas the depression time constant reduces it. The change in USE value is relative to both the facilitation and depression time constants. The USE value always lies between 0 (no efficacy) and 1 (full efficacy). The SSD doesn't result in a permanent change of the effectiveness of a synapse; when there are no new APs arriving at a post-synaptic neuron, the USE value of a synapse is recovered back to its original state.

The LSD or Hebbian learning has a permanent effect on the effectiveness of a synapse. This effect depends on the timing of the arrival of the pre-synaptic and post-synaptic APs. If a post-synaptic AP arrives after a pre-synaptic AP then the synapse that delivered the AP will be in a positive learning window and thus it gets strengthened. If a pre-synaptic AP arrives after a post-synaptic AP then the synapse that delivered the AP will be in a negative learning window and thus it gets weakened. If the pre-synaptic and post-synaptic APs arrive at the same time then there is no change in the USE value [7]. Figure 2.6 shows two pre-synaptic APs firing at different time periods. Figure 2.6A shows that during a positive learning window the synapses that fire to neuron N are strengthened whereas Figure 2.6B shows that during a negative learning window the synapses that fire to N are weakened.

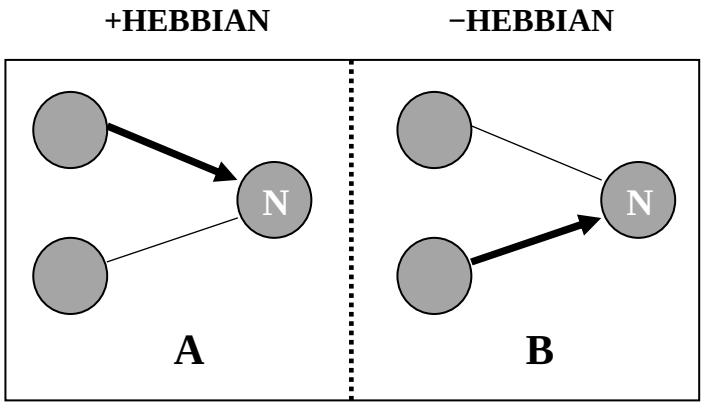

Figure 2.6 Positive and negative hebbian learning

Columns and Layers

The cortex present in a human brain is conceptually arranged into columns [56] wherein a complex neural connectivity is observed. This connectivity leads to efficient processing of information. Based on the size of both the cortex and the columns it is predicted that there are around 2 millions columns that can fit into the cortex of a human brain [44]. It is also assumed that there can be more columns in the case of overlaps [74]. The columns form a container for the layers which implies that the columns are further divided into layers. Most columns of the cortex have six layers. Layers in turn form a container for cells which are placeholders for the compartments. It is to be observed that there is no difference between the columns and layers in NCS; they are defined to hold a cell distribution. Once the layers have been filled with the cell distribution, a probabilistic model is used to establish the synaptic connections. The probability of connections within a layer is higher than the probability of connections between the layers and the least probability of connections is across columns. This organizational structure of columns, layers, cells, and compartments, and connections within and between layers and columns is used in the input file of the NCS to define a specific brain model. Figure 2.7 shows the structure of column-layer-cell arrangements in the primary sensory, association, and primary motor cortices.

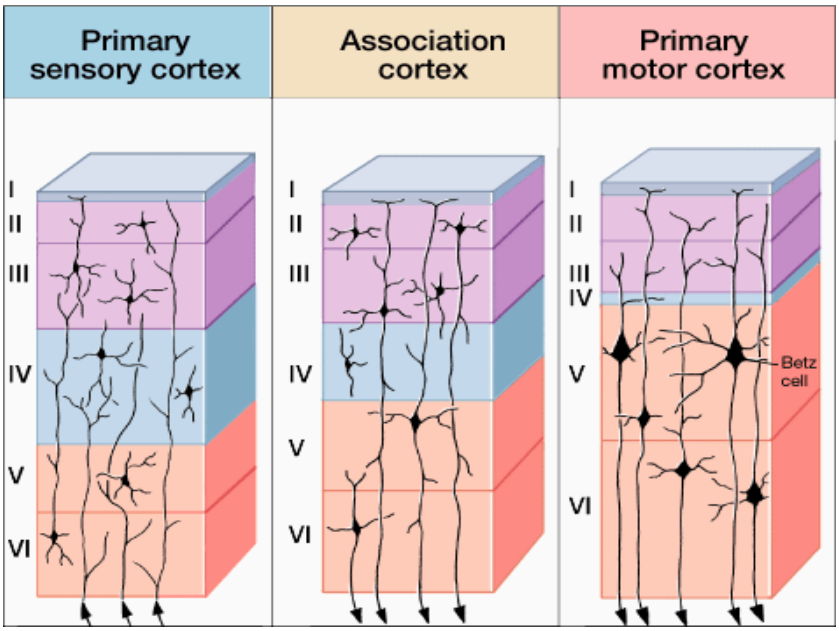

Figure 2.7 Column-layer-cell arrangements in the sensory, association, and motor cortices [9]

Compartments

As mentioned above, in NCS the cells form a container for the compartments and the spiking activity occurs within these compartments. The compartments in turn form a container for the channels and also keep track of parameters such as membrane potential and the type of channel used by the compartment. A cell can always have exactly one active compartment at any point of time even though it contains multiple compartments. The compartment generates a spike when the membrane voltage reaches a threshold value and propagates it to all other connected cells or compartments via synapses. The soma compartment of a neuron plays a role in keeping track of the membrane voltage, which is adjusted depending on the incoming current from other compartments or cells. The soma compartment receives electrical inputs from various other neurons and depending on whether the membrane voltage reaches a threshold, an AP is fired. This process of collecting electrical stimuli and producing an AP is termed “integrate-and-fire”. The propagation of information across the complex networks of a brain in the form of an AP generated by the cells or neurons is described in Hasselmo (1998) [38] and Koch (1999) [48].

Channels

The channels present in the compartment affect the flow of ions thereby causing the membrane voltage to either fire or suppress an AP. NCS is designed to model M, A, and AHP potassium channels that are abbreviated as K_M, $K_{A,}$ and K_{AHP} respectively. An M channel is activated when there is an incoming AP and its role is to inhibit the membrane voltage from reaching a threshold. An A channel is activated when the membrane voltage is in the process of reaching a threshold, but turns off on reaching the threshold [36]. An AHP channel is unlike the other channels and it is not voltage dependent. It is affected by the release of calcium (Ca^{+2}) into the compartment during firing of an AP. The release of calcium results in activating an AHP channel that hyperpolarizes the compartment thereby inhibiting additional firing.

2.2. Oxytocin and its Significance

OT is a neuropeptide hormone containing nine amino acid molecules present in a mammalian brain, is primarily produced by the hypothalamus (discussed later in this chapter), and acts as a neurotransmitter in the brain. It is also called an alpha-hypophamine or cuddle hormone. Specifically, it is called “cuddle hormone” because it plays a role in social recognition, pair bonding, and maternal behaviors (discussed later in this chapter). The OT that is released into the hypothalamus is synthesized by the hypothalamic neurons and is released into the posterior pituitary gland for secretion into the bloodstream. Apart from being released within the brain, the OT is also released by other tissues such as testes and ovaries. Figure 2.8 shows the structure of an OT hormone.

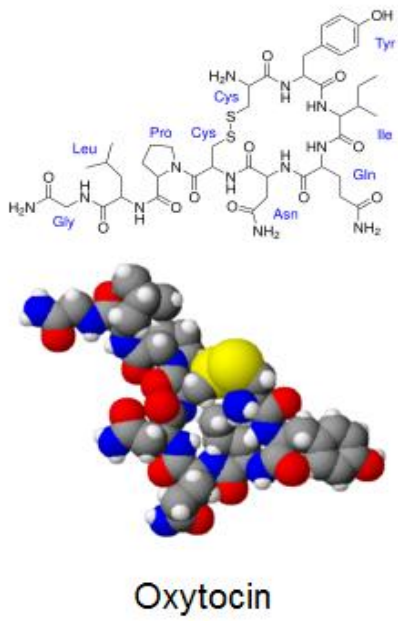

Figure 2.8 Structure of an OT hormone [11]

2.2.1. Female Reproductory System

OT is considered to be responsible for certain physiological functions in the female reproductory system such as serving to stimulate and regulate continuous contraction of the smooth muscle tissue of the uterus during labor [25], milk letdown for breastfeeding in lactating women [25], and sexual behavior [18]. A more detailed explanation of the role played by OT during labor and milk letdown is given below whereas the effects of OT on sexual behavior are still unclear.

1. **Contraction of Uterine Muscles:** In order for a women to deliver a child, during later stages of the gestation period there should be vigorous contraction of the muscle tissue of the uterus for a prolonged period of time. At the end of the gestation period, when a woman is ready to give birth to a child, there is an increased release of the OT receptors at the muscle tissue of the uterus, which causes irritation of the uterus and sometimes to the women as well. The release of OT is triggered by the child when it tries to stimulate the cervix and vagina during labor and it improves the contraction of uterine muscles thereby giving birth to a child. This process of giving birth to a child is called parturition.

2. **Milk Letdown:** In lactating women, the milk is initially released into alveoli (tiny sacs located within the mammary gland) and from there it is excreted through the nipples. During breastfeeding, when a child sucks the nipple of a woman, a signal is sent to the hypothalamus which causes the firing of APs by neurons that make OT and these APs stimulate the release of OT from the neurosecretory nerve terminals of the posterior pituitary gland. Thus, the OT release stimulates the contraction of the myoeithelial cells of the mammary gland thereby secreting milk.

2.2.2. Trust

Trust is an important aspect in our daily lives, playing a predominant role in social and personal relationships, financial matters, security applications, and many more [77]. Trust is said to be established when a person allows another person to make a decision that would in turn affect the first person's welfare. Trust develops when the trustee is increasingly predictable by the trustor because of experiences and interactions with the trustee. A typical real-world example of trust is observed in financial affairs where unless an investor gains trust of a banker, dealer, or stockholder, he or she is not willing to invest money.

OT is responsible for developing trust in the humans [21, 39, 41, 50]. It plays a key role in modulating complex emotional and social behaviors, social recognition, and aggression [19, 31, 32, 61, 68, 75, 76]. In addition to these, OT plays a crucial role in social bonding [51, 81] and improving short-term memory [28, 66].

Since OT has a considerable effect on the female reproductory system, it is widely used as a medicine for treating female humans. During labor, if the rate of contractions of the uterus is low or inconsistent then OT is infused into the body of a female which enhances the rate of contractions and generates rhythmic movements of the uterus. It also helps to stop bleeding of the uterus after a child is born. In addition, OT initiates a smooth abortion and regulates improper or inevitable abortion. Finally, it stimulates milk letdown in the lactating women suffering from improper excretion of milk during breast feeding and provides a treatment for breast engorgement (swelling) and mastitis (infection) [43].

Apart from the above mentioned general treatments, it also plays a role in complex cognitive functions. OT induced into the human body can enhance the feeling of trust [21, 39, 41, 50] and improve memory of recognizing faces [28, 66] that in turn results in social recognition [32, 68]. It is also predicted that OT may play a key role in treating people who are suffering from autism (refraining from social interactions) and social phobia (fear of social affairs or interactions) [17].

2.2.3. Hypothalamus

The hypothalamus is a cone-shaped component which is of the size of an almond present in the brain between the thalamus and the brainstem. The hypothalamus is located just below the thalamus and above the brainstem. The most important function performed by the hypothalamus is to connect the endocrine system to the CNS. The endocrine system is a collection of glands wherein each gland is responsible for the secretion of a specific type of hormone into the blood vessels to control the functioning of a human body. The functions regulated by the endocrine system are tissue function, mood, metabolism, and growth. The hypothalamus plays a prominent role in releasing essential neurohormones like Thyrotropin-Releasing Hormone (TRH), Gonadotropin-Releasing Hormone (GnRH), Growth Hormone-Releasing Hormone (GHRH), Corticotropin-Releasing Hormone (CRH), Somatostatin, Dopamine, Vasopressin, and OT. All these neurohormones secreted by the hypothalamus regulate hunger, thirst, sleep-wake cycles, emotions, body temperature, motor functions, homeostasis, and circadian cycles. Figure 2.9 shows the structure of a human brain with the hypothalamus.

OT is released from the dendrites of magnocellular neurons present in the Supraoptic Nucleus (SON) and the Paraventricular Nucleus (PVN) of the hypothalamus [52]. They are considered to be the main sources of OT release. The release of OT from the dendrites is considered to have an effect on the ventromedial hypothalamus and is also viewed as a possibility for the regulation of food intake [69].

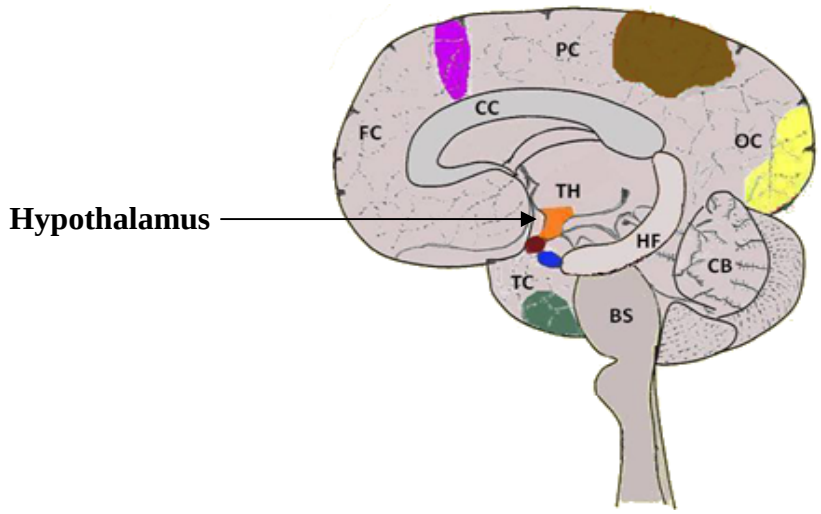

Figure 2.9 Structure of a human brain showing the hypothalamus

2.2.4. Amygdala

The amygdala is a component of the limbic system that plays a prominent role in emotional reactions and memory. There are two almond-shaped organs located in the medial temporal lobe of a mammalian brain which are termed amygdalae. The amygdala is particularly involved in the response to fear and it is believed that various disorders related to anxiety are a result of the amygdala function. The neurons present in the amygdala respond to different kinds of stimuli such as visual, auditory, taste, smell, and somatosensory. Among these stimuli, a high percentage of the neurons respond to the visual stimuli. Figure 2.10 shows the structure of a human brain with the amygdalae represented by red color.

The primary responsibility of the amygdala is to form memories of emotional situations and store them in the brain. It is understood that during fear conditions, when a sensory input is received by the amygdala, a memory of the stimuli is formed within the brain. Thus, a similar emotional experience would result in reinforcement learning and stronger excitation of fear which in turn causes long term memory of the emotional event.

During social interactions, OT has a profound effect on the amygdala. An increase in the level of OT would suppress the activity in the amygdala [47, 64], which is responsible for social cognition and fear in mammals [27, 59, 79], thereby establishing trust. During emotional events, OT is released into the hypothalamus and is directed to the amygdala where the effect of OT on the amygdala is observed. Significant release of

OT into the amygdala would result in suppression of fear [47, 64].

In biological experiments it is stated that removing the amygdala from the brain would result in loss of fear. A rat "will walk up to a sleeping cat and even nibble on its ear" if the amygdala is removed from its brain [20].

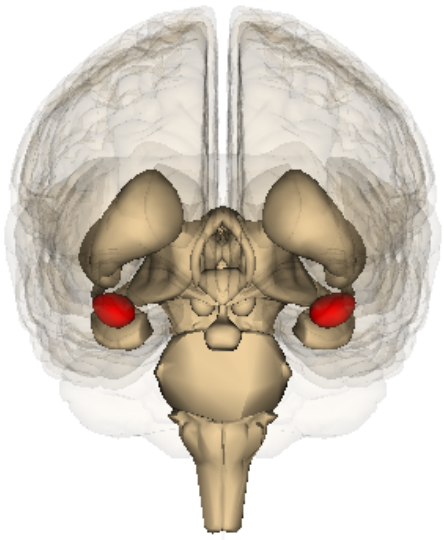

Figure 2.10 Structure of the brain with the amygdala [3]

2.3. Sensory, Motor, and Association Areas

In the mammalian brain, the cerebral cortex is referred to as a layer that covers the outer region of the cerebrum. It holds two-thirds of the mass of a mammalian brain and is divided into two hemispheres called the left hemisphere and the right hemisphere. It is a highly developed component of the mammalian brain and is responsible for complex cognitive functions such as attention, memory, consciousness, thought, perception, and language.

Processing of information primarily occurs in the cerebral cortex. This cortex can receive input from all the sensory organs and there are specialized processing units in the cerebral cortex for different kinds of stimuli such as visual, auditory, tactile, smell, and movement. It also contains areas which are capable of performing higher cognitive functions such as thinking and reasoning. Most of the functions are performed in both the left and right cerebral hemispheres whereas certain functions such as language processing are performed in only one hemisphere. Figure 2.11 shows the cerebral cortex of a human

brain with different areas responsible for processing information.

The cerebral cortex is primarily composed of three areas: sensory, motor, and association areas. They are described as follows:

Sensory Area: This area receives inputs from various sense organs and process the information. The regions present in the cerebral cortex that receive sensory stimuli directly from the thalamus are referred as primary sensory areas. The visual, auditory, and tactile sensory inputs are served by the primary visual cortex, primary auditory cortex and primary somatosensory cortex, respectively. It is understood that most of the time information from the sense organs present on the left side of the body is received by the right hemisphere and information from the sense organs present on the right side of the body is received by the left hemisphere. For example, the visual input from the left eye is received by the right visual cortex.

Motor Area: This area is located on either side of the brain in both the left and the right hemispheres. The primary motor area is responsible for performing muscular movements as a result of the sensory stimuli received by other areas of the cerebral cortex. It plays a prominent role in coordinating the sensory inputs with the motor actions. The primary motor area is generally responsible for voluntary movements. An electrical stimulation of the motor area in the right hemisphere results in the movement of limbs present on the left side of the body. According to the structure and function of the primary motor cortex, it is well understood that the primary motor cortex is associated with Brodmann area 4 and Brodmann area 6. These areas are believed to play a role in the planning of complex, coordinated movements.

Association Area: This area plays a role in complex cognitive functions such as memory, attention, language, and thought. The primary responsibility of the association area is to build a map of the environment based on the sensory stimuli and facilitate the human to interact effectively which results in attention and memory. During the process of interaction, the association area might play a role in language and thought. Sensory inputs are received by parietal, temporal, and occipital lobes that are responsible for creating a meaningful representation of the environment and the frontal lobe is associated with planning the actions and movements of the human.

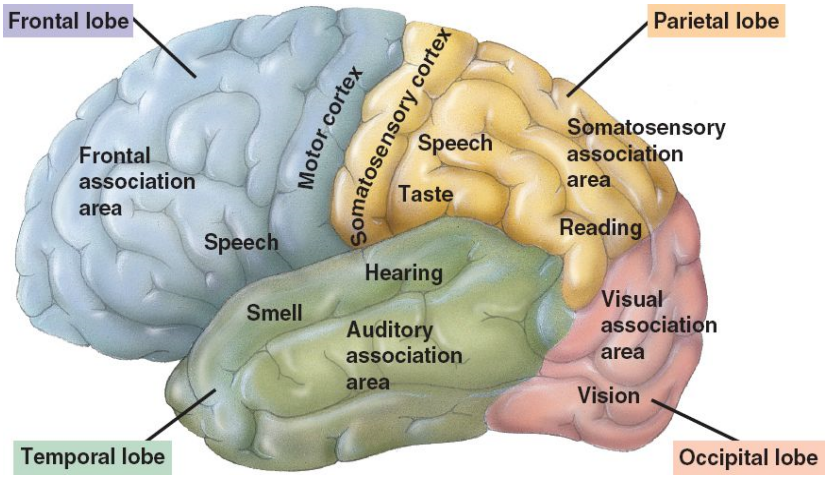

Figure 2.11 Cerebral cortex of a human brain [4]

2.4. Brainstem

The brainstem is located at the rear portion of the brain and extends down in order to connect to the spinal cord. Its primary responsibility is to relay information between the brain and the rest of the body. It also plays a vital role in functions such as cardiac and respiratory systems along with regulating the sleep cycle and maintaining consciousness. The brainstem is divided into three segments called medulla oblongata, midbrain, and pons. Figure 2.12 shows the structure of the brainstem with its three segments.

Medulla Oblongata: It is located at the bottom of the brainstem and functions as a medium for transmitting motor information between the brain and the spinal cord. Medulla oblongata contains centers for cardiac, respiratory, and vasomotor functions and regulates motor actions such as swallowing, coughing, and vomiting.

Pons: It is located between the medulla oblongata and the midbrain, and functions as a bridge between the different parts of the brain. Pons helps in the transmission of information from the medulla oblongata to the higher cortical columns of the brain. Also, it contains the center for the respiratory function.

Midbrain: This is the topmost part of the brainstem and serves as a neural pathway for the left and right cerebral hemispheres. It contains centers for visual and auditory functions.

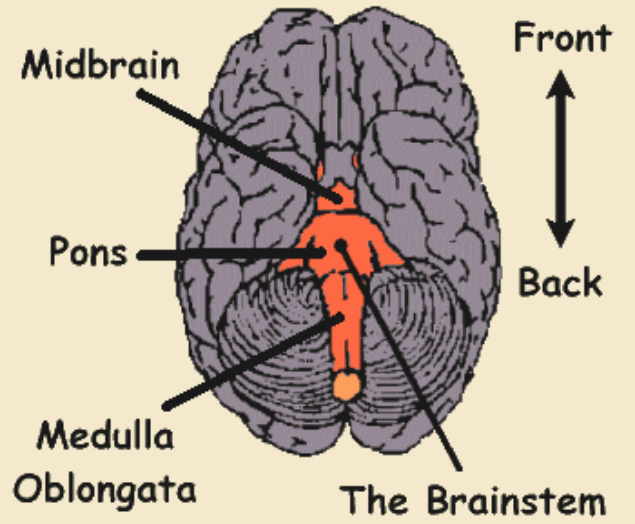

Figure 2.12 Brainstem [2]

Chapter 3: Technical Background

3.1. Brain Simulators

In order to computationally model the neural systems of a biological brain exhibiting spiking activity there are a variety of widely used simulation tools available. A few of them are as follows:

NEURON

NEURON [24] is a simulation tool developed by John W. Moore and Michael Hines at the Duke University. It is used to model neurons and the neural circuitry of a brain based on the true biological properties, observed during *in vivo* recordings. The current version of NEURON is capable of constructing and simulating large-scale neural systems efficiently where the biological properties of cells play a prominent role. It provides a greater flexibility of modeling certain key aspects of cells such as the extracellular potential near the membrane, several channel types, irregular channel distribution, ionic diffusion, and accumulation.

The advantage with NEURON is that it is provided with a sophisticated Graphical User Interface (GUI) that contains a collection of tools to create models, run simulations, and analyze results. Hence, no knowledge of programming is required. It is a well designed simulation tool wherein its GUI contains model specification tools: channel builder, cell builder, network builder, linear circuit builder; model analysis tools: import3D, model view, impedance; and simulation control tools: variable step control, multiple run fitter.

GENESIS

GENESIS [24] is a simulation environment developed by James M. Bower at California Institute of Technology. It is capable of modeling biologically realistic neural systems with functionalities ranging from the subcellular components to complex models involving single neurons and large networks of neurons. Complex models of neural systems can be constructed by adding the required functionality to the existing reusable objects without the need to comprehend, modify, and recompile the simulator code.

GENESIS also supports a parallel simulation environment in order to model large scale networks on a cluster, supercomputer, or network of workstations that support Message Passing Interface (MPI).

To construct the individual or networked neuronal models, customized script files are written that make use of the pre-compiled objects of GENESIS and are parsed by an interpreter. The advantage of using an interpreter is that the simulation can be modified or functionality can be added to an existing model while the simulation is still running. This can be achieved by passing the script files and without having to recompile the scripts into binary code which indeed doesn't affect the simulation speed. An additional advantage is that it is provided with 268 scripting language commands and 125 object types to make it rich and powerful, so that only a few lines of script are required to add custom functionality to a simulation.

NEST

NEST [24] is a project started by Markus Diesmann and Mark D. Gewaltig to make use of the technology advancements in building a neural network simulator that is capable of modeling large-scale neuronal networks resembling biologically realistic connectivity. It easily accommodates a network size of 100,000 neurons wherein each neuron is provided with a significant number of synapses and can have either single or limited number of compartments. It also supports different synapse types and neuron models. It supports parallelization by message passing and multi-threading wherein a simulation can be distributed over a cluster of computers or multiple processors of symmetric multiprocessing architecture.

The advantage with NEST is that it is designed to produce the same simulation results with the same network for any number of trials irrespective of the number of processors on which the simulation is run. Moreover, there is a high-level of modularity in the code of NEST which assists in adding new functionality at runtime to construct new neuronal models or decoupling existing functionality from the code during the later releases of NEST.

NCS

NCS is a massively parallel software program running on a shared-memory 48-processor Sun Fire X4600 cluster that is capable of modeling the biologically realistic neocortical NN. Absence of parallel architectures, need for simplification of degree of neuronal compartments for better performance, discovery of interesting details related to synaptic plasticity, and connectivity led to the development of NCS which was responsible for modeling horizontally dispersed, vertically layered distributions of neuronal properties of the mammalian neocortex. NCS is programmed to accommodate leaky integrate-and-fire neurons which are characterized by a membrane time constant (20 ms), a membrane resistance (100 MΩ), and a resting membrane potential (-60 mV) with conductance-based synapses. The sampling frequency of a conductance-based synapse is 1,000 Hz per second. An AP is fired when the membrane potential reaches a threshold of -50 mV and later switches back to the resting potential. NCS is designed to compute a reordered form of the Hodgkin-Huxley model at a single cell level by adding a constant membrane leak during the numerical integration, which is represented by equation (1).

$$C_N \frac{dV}{dt} - I_M - I_A - I_{AHP} - I_{input} - I_{syn} - I_{leak} = 0 \qquad (1)$$

Both I_M and I_{AHP} contribute to the membrane voltage by controlling spike-frequency adaptation. These are small ionic currents that have long period of activity when the membrane voltage is between rest and threshold. Mostly used in this study, I_{AHP} is the current provided by small spike-adaptation contributing channel. These represent voltage independent K^+ channels that are regulated by internal Ca^{2+}, where the charge delivered after each time step is updated as:

$$I_{AHP} = g_{AHP} S m^P (E_{AHP} - V) \qquad (2)$$

where *S* is a non-dimensional strength variable added to the NCS and *P* is the power that the activation variable *m* is raised to. This K_{AHP} *m* particle is modeled as:

$$\frac{dm}{dt} = \frac{m_\infty - m}{\tau_m} \qquad (3)$$

$$\tau_m = \frac{\epsilon}{f(Ca) + b} \qquad (4)$$

$$m_{\infty} = \frac{f(Ca)}{f(Ca) + b} \quad (5)$$

where is the scale factor, *b* is the backwards rate constant, and *f(Ca)* is the forward rate constant defined by:

$$f(Ca) = k[Ca]_i^{\alpha} \quad (6)$$

where α is the exponential factor.

Internal Ca^{2+} concentrations are calculated at the compartment level in the NCS. Physiologically, the concentration at a cell increases when an AP fires. After the AP has ended the internal concentration of Ca^{2+} will diffuse through the cell, where it is taken up by numerous physiological buffers. In the NCS, this diffusion/buffering phenomenon is modeled by a simple decay equation:

$$[Ca]_i(t+1) = [Ca]_i(t)\left(1 - \frac{dt}{\tau_{Ca}}\right) \quad (7)$$

where *dt* is the stimulation time step, and τ_{Ca} is the defined time constant for the Ca decay.

The synaptic currents are calculated by:

$$I_{syn} = g_{syn} PSG(t)\left(E_{syn} - V\right) \quad (8)$$

The leakage current is voltage-independent and is modeled by:

$$I_{leak} = g_{leak}(V - E_{leak}) \quad (9)$$

Notice that the driving force is expressed using the normal convention. This is the reason why the leakage current is subtracted in the membrane voltage equation rather than added, as seen in the traditional membrane voltage equations.

I_{input} is used to ignite networks when it is appropriate to do so by receiving external input and I_{syn} corresponds to excitatory and inhibitory afferents neurons. Reversal potentials for excitatory synapses are E_{AHP} = -80 mV, E_{syn} = 0 mV and for inhibitory synapses it is -80 mV. The resting membrane potential is E_{rest} = -60 mV.
Synaptic conductances (g) are computed using:

$$\tau_s \frac{dg}{dt} = -g \qquad (10)$$

with $g \leftarrow g + w_i$ upon the spike arriving at synapse i

There have been five different versions of NCS release over a period of 13 years starting from its inception in 1997. A discussion about each version's characteristics follows:

NCS1 and NCS2

The first version of NCS, called NCS1 [83], examined the possibility of modeling experimental results collected from the rat brain slices using MATLAB as the development environment. NCS1 was capable of modeling calcium dependent AHP channels, voltage dependent A and M channels, along with the implementation of synaptic delay and membrane impedance. The simulation results were compared to the observations from biological studies. Based on the published results from Markram and colleagues [73], adjustments to short-term and LSD because of regulation of synaptic efficacy by Hebbian were included. Testing was done on a simple model with 2-column architecture and a single compartment containing 160 neurons. The result of correlation between input-output pairs was observed.

Though the MATLAB basis of NCS1 showed promising results, it was running slow because of serial interface i.e., it didn't have the capability to run on multiple processors simultaneously thereby restricting its ability to simulate larger numbers of cells and synapses in a network. In order to run large scale simulations efficiently, the C version of NCS, called NCS2 [83], was developed with capabilities for parallelism included. To analyze the performance of NCS2, experiments were carried out on a 20 node Beowulf cluster composed of 450 Mhz Pentium CPUs with an increase in the network size from 100 to 1,000 cells and the number of CPUs from 1 to 10. An optimum number of CPUs used for running the simulation efficiently was 10 and anything beyond that did not result in a better performance for NCS2.

Figure 3.1 shows a boost up in the performance of NCS2 for a 1,000-neuron simulation running on increased number of CPUs. The large difference in speedup between the ideal and actual results was a result of slow switching across the Ethernet.

The next version of the NCS included a high-speed Myrinet switch and faster CPUs. This development had resulted in simulation of complex biological NNs.

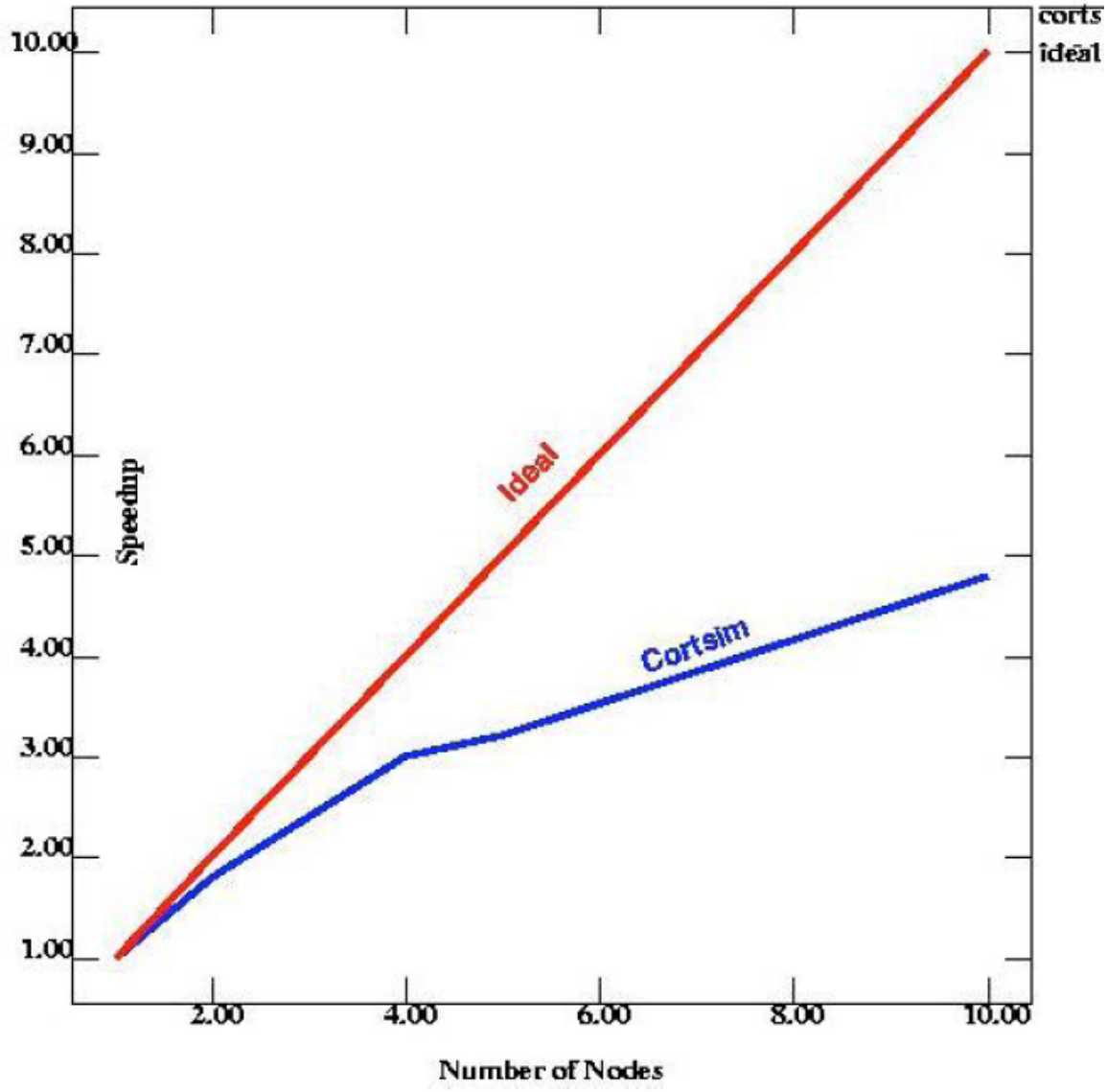

Figure 3.1 Performance boost of the parallelized NCS2 [83]

NCS3

The third version of NCS, called NCS3 [83], was developed in C++ and utilized the full power of object-oriented design principles to produce refined code structure and performance [80]. The advantage of using C++ was that all the neuronal properties of the brain models and the relationships among them could be broken down into objects. This led to the accomplishment of two objectives. First, since the objects were fully

encapsulated various implementations were possible based on the existing objects by adding, removing, or modifying portions of the code without having to rewrite everything from scratch. This resulted in easier and efficient implementations and enhancement of neuronal properties of complex brain models. Second, the objects could serve as containers for other objects, thus allowing for a better organization of the code. Examples where the objects serve as containers are the column objects serving as containers for the layer objects, the layer objects serving as containers for the cell objects, and the cell objects serving as containers for the compartment objects.

NCS3 was a C++ version of the original NCS with additional features that have been completely rewritten from scratch. The goal of NCS3 was to allow for ease of maintenance and future enhancements of the code along with the ability to run simulations on multiple CPUs simultaneously. NCS3 used the MPI API for the purpose of parallel execution of an NCS simulation on a cluster of CPUs. MPI assisted the cell groups, which were equally distributed on the nodes of the cluster, to communicate spike messages among them via the Message Bus. In NCS3 the Message Bus object was responsible for regulation of information flow between objects on and off a node. This indeed resulted in proper timing and synchronization of simulations thereby preventing deadlock and starvation. The interaction between the Message Bus object and various components of NCS3 is shown in Figure 3.2.

In addition to software refinements, a great deal of improvements were done to the hardware as well [83]. To improve the efficiency of the simulator and to run complex models, the *cortex* cluster was introduced, which consisted of 30 dual-Pentium III (1GHz) processor nodes with 4 GB of RAM per node. The installation of a Myrinet switch resulted in higher data transfer rates without choking the network, as opposed to Ethernet, since Myrinet uses an efficient packet switching technology. Thus, with the introduction of the Myrinet switch the simulation speed improved significantly.

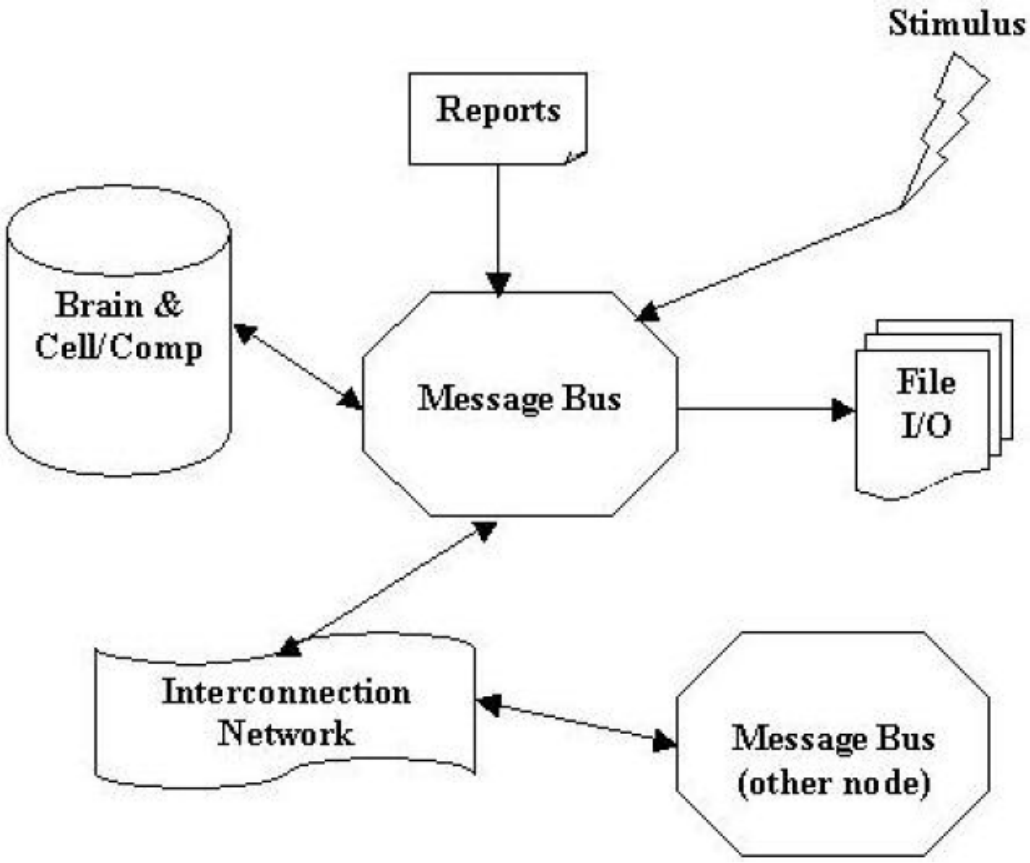

Figure 3.2 Communication model of NCS3 with emphasis on the message bus object [80]

To make use of the channel structures, located within the compartments of the cells, and demonstrate accurate dynamics of inter-neuronal GABAergic systems, experiments were performed using NCS3 [83]. It supported modeling M, A, and AHP potassium channels. The observations from previously published *in vitro* experiments after applying one second step currents in the range of 50 to 350 pA were mimicked using NCS3 by properly combining the channels. The results of mimicking the behavior of various neurons by NCS3 are shown in Figure 3.3. The various types of neurons are classic nonaccommodating (cNAC), classic accommodating (cAC), bursting non-accommodating (bNAC), bursting accommodating (bAC), delayed non-accommodating (dNAC), delayed accommodating (dAC), classic stuttering (cSTUT), and bursting stuttering (bSTUT). The behaviors of various types of neurons, excluding “stuttering”

types, were relatively robust under a two-fold variation in strength for a single somatic cell [53].

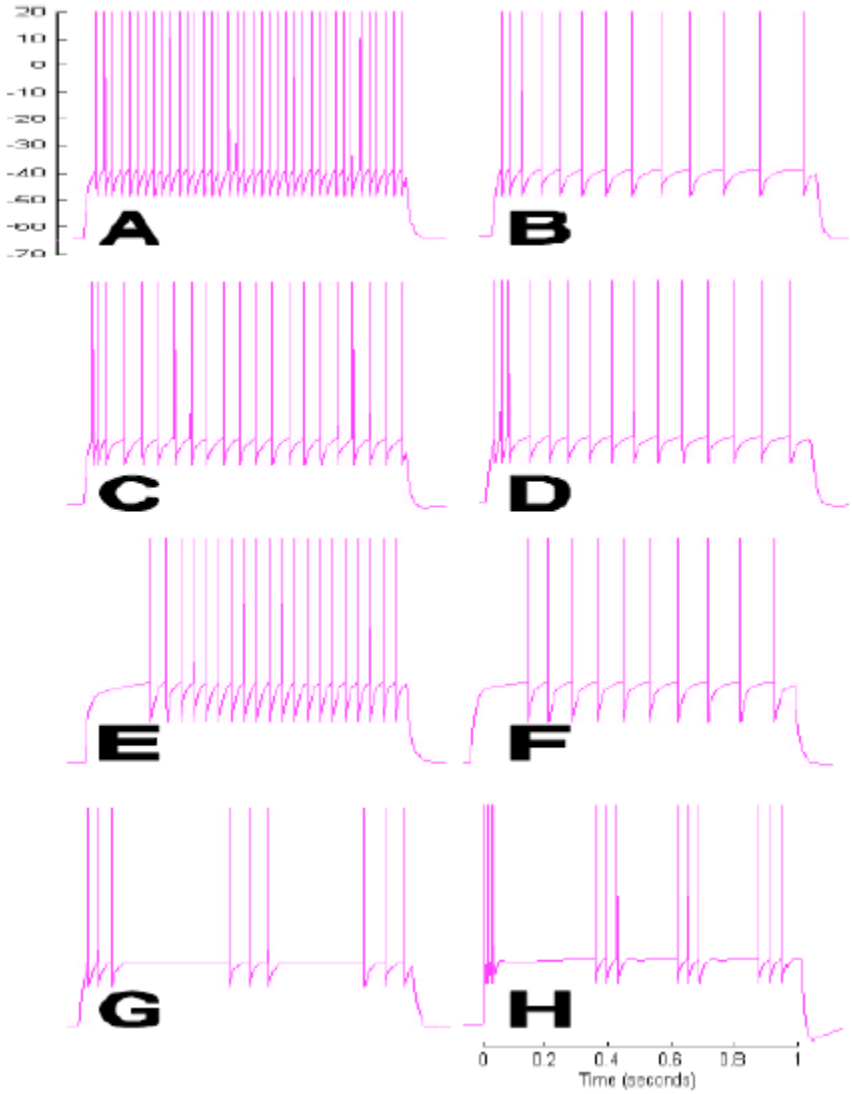

Figure 3.3 Simulated response to 1 second step current from 150-300 pA [53]
(A) cNAC (B) cAC (C) bNAC (D) bAC (E) dNAC (F) dAC (G) cSTUT (H) bSTUT

NCS4 and NCS5

The subsequent versions of NCS, NCS4 and NCS5 [83], provided better performance and speed optimizations along with elimination of bugs and errors from the code. This resulted in more stable and reliable versions. The previous versions of NCS supported neurons with only one soma compartment that were referred to as point neurons whereas the later versions supported creation of complex cells containing several

compartmental structures such as axons, spines, and dendrites. An added functionality to the newer versions of NCS was the capability to assign geometric information to the structures. For example, the probability of connections between synapses among closely spaced objects is higher. Similarly, the speed at which an AP travels is faster for closer destinations. The ability to save the state of a brain model and reload it without having to run the whole simulation again was incorporated, which resulted in reuse of synaptic dynamics, affected by Hebbian learning of a previous simulation, for future simulations.

In addition to the above mentioned refinements, several optimizations related to the simulation speed of NCS were made. The concept of load balancing played a prominent role in order to improve the speed. The challenge associated with load balancing is to make sure that all the processors distribute the tasks equally among themselves and there is no burden on a few processors while the others are idle [33, 34]. In NCS3, the cells were distributed uniformly over the cluster whereas in NCS4 and NCS5 the synapses were of primary focus in order to have a balance of work on the cluster. Since, synapses needed a large share of memory during the simulation it was essential to distribute total number of synapses on the cluster. With the optimization of connection process the time taken to initialize a brain network was reduced. The previous versions of NCS checked for all possible connections and the probability of each connection before initializing a network. This approach resulted in a time complexity of $\boldsymbol{O}(n^2)$, where n represented the total number of cells that can be connected among themselves in the network. The latest versions determine the desired number of connections and randomly choose available cells to create a connection between them. The time complexity for this approach is $\boldsymbol{O}(n)$. Additional optimizations included decreasing the overhead on the Message Bus by reducing the size of message packets that resulted in faster delivery of these packets to their destinations. Figure 3.4 shows a graph comparing the speedup in the NCS simulation to that of an ideal state after dealing with the latest optimizations. The inset graph represents the same data on a logarithmic scale.

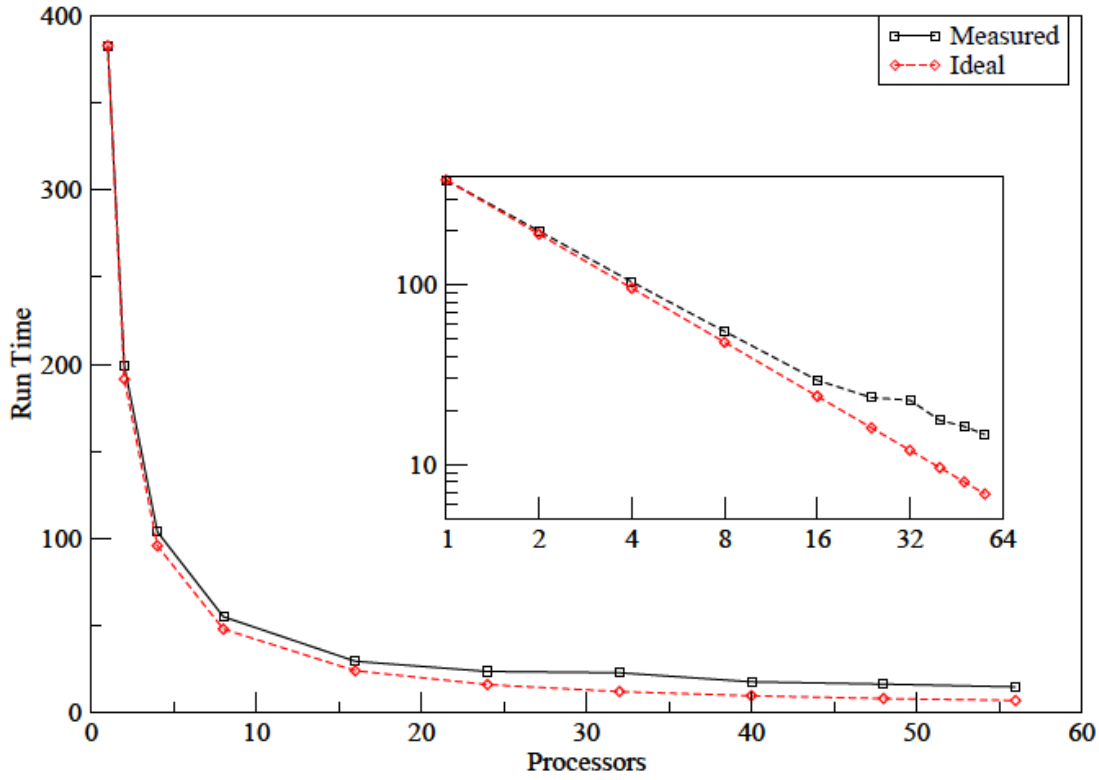

Figure 3.4 Graph showing the speedup closer to ideal, after optimizations to NCS [33]

With the aid of the latest versions of NCS numerous biological experiments were performed. One of these experiments analyzed how information may be encoded by spike-timing and membrane dynamics of biological neurons [83]. Comparisons were made between the biologically influenced NCS and ANNs (Artificial Neural Networks) in order to emphasize that NCS was superior in terms of flexibility and robustness. The latest version of NCS also supports sensory modalities such as vision and audition in accordance with the humans and plays a prominent role in situations that require pattern recognition and speech perception.

Another noticeable experiment was the investigation of intracortical and cortical-subcortical “networks of networks” that are involved in attention, memory, emotion, reward, sensory-motor association, motor movements, and theory of mind [67]. The goal of this experiment was to comprehend the interactions between these modules with the NCS providing a base for experimentation. The analysis of current research led to the development of complex brain models with neurons ranging from 1,000 to 1,000,000.

These brain models were capable of sustaining auditory patterns with stability. The simulation resulted in a large interconnected network because of 600 million synapses.

3.2. Robotics

Robotics is a scientific and research field that deals with the design, construction, and implementation of machines as an aid to human beings in various fields of activity. Currently, robots are extensively operated in the automobile industries to perform repetitive tasks. Apart from that, they are also being used in the medical field to assist in surgeries [26], fire fighting [37], entertainment [54], law enforcement [58], and so forth. In general, social robots play a prominent role in assisting human beings.

3.2.1. Artificial Intelligence

During the initial stages of the development of social robots, since the tasks to be performed were simple enough, classical methods were used to train the robots to assist the human beings. As time progressed, there was a need to make robots operate in complex and unknown environments by preparing them to learn and adapt to the new environments. The concept of AI was introduced at this point. AI consists of methods such as Neural Networks (NN), Fuzzy Logic (FL), and Evolutionary Algorithms (EA).

Neural Networks: They represent complex interconnected networks that serve as massively parallel computational engines. NN are highly adaptive and generally slow because of large number of connections. They are being used to predict non-linear and time-varying systems that have high randomness.

Fuzzy Logic: It is a mathematical formulation of a set of abstract ideas that can result in better implementation solutions. It is a powerful problem-solving technique used in information processing and embedded control. FL results in a close to precise solution from ambiguous, abstract, vague, and imprecise information. It is similar to the human brain in decision-making since the human brain analyzes vague information and produces appropriate solutions.

Evolutionary Algorithms: Inspired by the mechanics of biological evolution, they are used to generate global optimization solutions to various problems. EA are search

methods that differ from classical methods in the sense that a population of solutions is explored as opposed to a single solution in traditional methods.

Each of the above mentioned methods is reasonably capable of solving problems related to robot navigation based on some complex parametric estimations. But, there is still a need to develop intelligent robots that serve real world problems which require learning and memory capabilities. Because of the limitations of the AI methods, the focus of research has shifted to modeling biological NN.

3.2.2. Neuromorphic System

This refers to the implementation of sensory and neural circuitry on analog, digital, or combination of both (analog and digital) circuits that are present on very-large-scale integration systems. A neuromorphic system is based on the neurobiology of the brain and this could result in artificially developed real-time information processing systems that could further compete with human sensory system. Learning and memory can be modeled using the neuromorphic systems that could result in the development of intelligent agents. The neuromorphic systems are considered to be intelligent when compared to the systems built using traditional AI methods.

3.3. Webots

The webots is a professional mobile robot simulation software package developed by Cyberbotics Ltd. and is used by over 700 universities and research organizations. It offers a fast prototyping and simulation environment that supports modeling 3D passive objects or active objects called mobile robots. These robots can be developed with different locomotion schemes such as wheeled, legged, or flying robots. A 3D environment called world (.wbt) can be modeled with built-in *Scene tree* window using Virtual Reality Modeling Language (VRML). The webots software uses the Open Dynamics Engine (ODE) library for accurate physics simulation such as setting up mass, density, inertia, and friction coefficients, for both passive and active objects. This software package includes a complete library of sensors and actuators that are present on most of the mobile robots, including accelerometers, cameras, connecters, differential wheels, distance sensors, emitters, receivers, servos, and touch sensors. The sensors’

sensing range and accuracy, and the actuators' physical constraints resemble real world sensors and actuators. The webots software contains a large number of robot models such as AIBO, Nao, Bioloid, e-puck, Hemisson, Khepera, and Pioneer. Programming a controller for each of these models can be achieved in one of the supported programming languages, including C, C++, Java, Python, MATLAB, and Universal Real-Time Behavior Interface (URBI). Furthermore, it runs on multiple platforms such as Windows, Linux, and Mac OS and provides a number of interfaces to real mobile robots, so that once the simulated robot works as expected, the controller code can be transferred to a real robot such as AIBO, Nao, e-puck, Khepera, or Hemisson. The software is also useful in capturing screenshots and recording movies of the simulation in AVI or MPEG formats. Both simple worlds containing a single robot to complex environments with multi-agent systems can be simulated and effective communication between multiple agents can be established using the webots software.

To run a webots simulation an existing robot model has to be used or a customized mobile robot has to be built. To build a customized mobile robot and passive objects in the environment basic knowledge of 3D computer graphics and VRML97 are required. Once the robot and simulation environment are built, the robot controller has to be programmed using one of the supported programming languages. If the simulated version of the mobile robot is working well then it can be transferred to the real mobile robot. The entire scenario is shown in Figure 3.5.

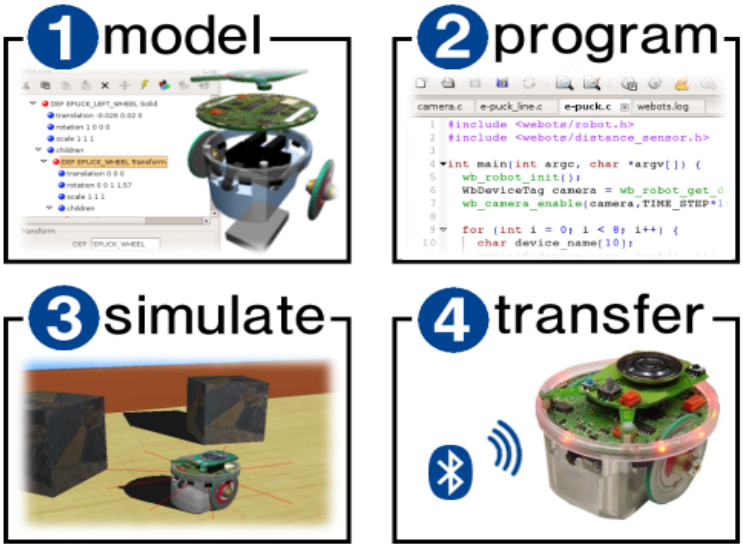

Figure 3.5 Running the webots simulation [16]

The webots software needs two important things to run a simulation: the world file and the controller program. The world file contains a 3D description of the mobile robot as well as the simulation environment whereas the controller program tells the robot to perform a specific action/scenario.

A world in webots is a 3D description of the properties of robots and all the objects present in the environment. This contains the description of every object's properties in the environment, such as the position, orientation, geometry, appearance, and physical characteristics. A world is organized as a hierarchical structure wherein objects might further contain other objects, e.g. a robot can have wheels, servos, sensors, camera, etc. A world file doesn't contain any code to operate the robot but it specifies the name of the controller to be used by each robot.

A controller is a program associated with the robot that can issue a set of commands to the robot for performing specific actions/scenarios. There could be any number of robots using the same controller but a separate process is started for each of them. A controller can be programmed in any of the programming languages supported by the webots software. Among these languages C and C++ need to be compiled; whereas Python, MATLAB, and URBI are interpreted. Java is both compiled and interpreted.

Chapter 4: Experimental Design

4.1. Overview

This chapter presents a detailed explanation of the ITI paradigm and the individual components required to run the simulation. It also describes the Virtual Humanoid Neurorobot (VHNR) that was designed using webots software. In addition to computational aspects, it also talks about the parts of the brain that have been modeled and play a prominent role in establishing trust. A brief description of each part is provided.

4.2. Intent Recognition

In social interactions trust is associated with recognizing intent of the communicating partner. There is an essential need to recognize the intent of others before making a decision since the result of our actions can offend the communicating partner. Intent recognition is a wide research area in robotics since it is very important to develop social robots that can cooperate with humans in performing various tasks [45, 71]. Understanding the intention of a person is essential for a robot to know what a human is expecting it to do. Often, the intention of a person can be represented explicitly by visual or auditory stimuli. For social robots to operate in the human world, intent recognition plays a key role and the importance of it can be understood from real world examples such as: for a robot-controlled car to travel on roads, it needs to understand the intentions of other drivers and also let the other drivers know about its own intentions by giving appropriate signals to avoid accidents; during military operations such as anti-terrorist activities robots have to determine the intentions of the enemy in order to prevent them from performing illegal activities; if robots are supposed to guard the society from anti-social elements then there is a crucial need for them to sense the intentions of people in order to resolve whether anyone is going to create any damage to the society; and, for robots to assist humans in industrial work, they need to know what humans expect from them to do.

4.3. Virtual Humanoid Neurorobot

The VHNR is a child-like Mobile, Dexterous, Social (MDS) robot which was custom-designed with the ODE for accurate physics simulation using Webots Pro 5.10 [16] and the URBI parallel-scripting engine [15]. The VHNR is a part of the Virtual Neurorobotics (VNR) framework and the design of it is quite simple, with just the torso or upper portion of the body and the differential wheels, in place of legs, to support locomotion. The VHNR is equipped with 55 servos, a differential wheels node, and a hidden camera located at the temple area. It moves the servos at a rate similar to human-like speeds. It has a total of 55 degrees of freedom (DOF) of which 3 DOF (vertical, horizontal, and tilt) are used for the neck with 30 degrees motion, 2 DOF (vertical, tilt) for each eyebrow and eyeball, 1 DOF (vertical) for each eyelid, 1 DOF (dilate/constrict) for each pupil, 2 DOF (left and right rotation) for torso with 30 degrees motion on the base, 18 DOF for right and left hand, and 1 DOF for teeth and mouth (open/close). The eyeball has a 30 degrees vertical and horizontal motion, shoulders with 90 degrees abduction and 45 degrees flexion, elbows with flexion from 180 degrees (straight down) to 30 degrees (hands close to the face) and wrist with 180 degrees inward rotation.

A servo can be of two types: linear and rotational. A linear servo position represents the distance between the servo's initial and current translation whereas a rotational servo position represents the difference between the servo's initial and current angle of rotation field. Each servo has certain limits beyond which it cannot move. There are two types of limits: soft limits and hard limits. Soft limits specify the software boundaries and if the target position is set beyond these limits then the position would be clipped off in order to fit into the soft limits' range whereas hard limits represent the physical or mechanical boundaries that cannot be overrun by any force and they are controlled by the ODE. Always, the range of soft limits should fall within the range of hard limits.

The VHNR controllers are programmed using the URBI and C++ to perform basic motor sequences such as the robot holds a rod and moves it vertically up and down (pounding) and horizontally back and forth (poking), it grabs a dumbbell and either hands it over to a person (trust) or pulls it back towards itself (distrust), and expresses happiness during trust and extreme anger during distrust. The robot was also configured to perform

head gestures such as nodding and shaking. The robot controller for the VHNR is a multithreaded C++ program that communicates with the brainstem using an internet protocol. A camera in real world acts as a robot eye to provide the visual stimulus. This stimulus is sent directly to the visual cortex of the brain and the parietal stimulus is sent to the parietal cortex of the brain by the VHNR via the brainstem.

4.3.1. Sony PS3 Eye Camera

A Sony Play Station 3 (PS3) Eye camera supporting frame rates of 60 hertz at a resolution of 640x480 and 120 hertz at a resolution of 320x240 is used to detect the motion of a human in the real world and send visual stimuli to the neuromorphic brain. In this study, the camera captures visual frames at a rate of 10 hertz. There are three visual cortical columns i.e., the vertical, horizontal, and reach columns that receive stimuli from the camera. The FOV of the camera is divided into four quadrants; vertical and horizontal motions are performed in the top two quadrants and reaching for an object is performed in the bottom two quadrants. The reason for this is to distinguish between the learning and the challenge phases. If a rod is moved vertically up and down by the human in front of the camera and the orientation of the Gabor filter is set to zero degrees then a visual stimulus is sent to the vertical column of the visual cortex since the Gabor filter is configured to detect vertical edges. Similarly, if a rod is moved horizontally back and forth by the human in front of the camera and the orientation of the Gabor filter is set to 90 degrees then a visual stimulus is sent to the horizontal column of the visual cortex since the Gabor filter is configured to detect horizontal edges. A visual stimulus is sent to the reach column of the visual cortex when the human reaches for an object that is placed on a table with the orientation of the Gabor filter set to 90 degrees.

4.3.2. Gabor Filter

The Gabor filter [13] is used to process the images of a human’s motion thereby representing the activity of the moving edges in the V4 region of the visual cortex. The activity generated by the Gabor filter closely resembles how the visual information is processed in the mammalian brain. It performs spatial filtering of an image based on frequency and orientation, and is often used for edge detection. Although Gabor filters provide an excellent approximation of the human visual information, they are

computationally expensive for real-time applications. In order to improve the processing speed, the Gabor filter application was developed on a Graphics Processing Unit (GPU) with NVidia's CUDA programming environment.

The image processing mechanism is described in Figure 4.1 wherein the processing begins with the capture of a 320x240 pixel image at a frequency and orientation that is specified by the user during the application configuration. A 128x128 pixel area of interest is then selected and the grayscale information is extracted from the selected portion. The extracted portion or area of interest is differenced from the previously captured image thereby providing an immediate representation of the motion between the two images. This resembles the neuronal properties of visual information processing in the V1 cortical area [60]. The differenced image is then padded with zeros in order to generate a 256x256 pixel image and a fast Fourier transform (FFT) is computed. The image in the frequency space is processed with a precomputed complex Gabor kernel and the inverse FFT is computed. The original 128x128 pixel area is extracted and segmented into a user-defined number of regions. Each region is normalized and averaged, and then sent to the running NCS brain simulation using the network interface.

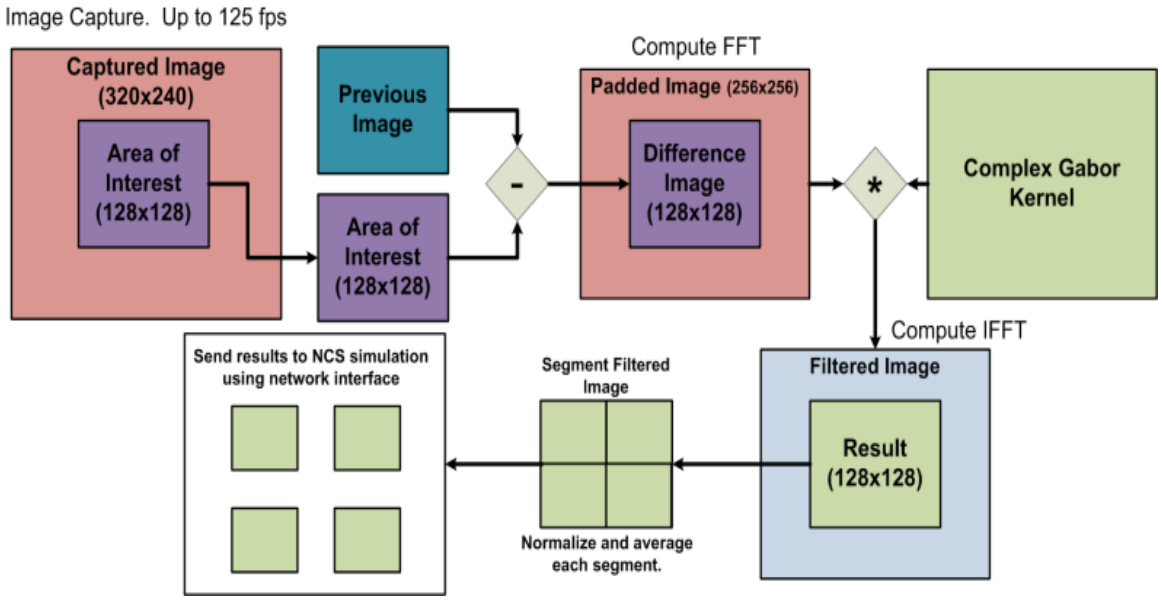

Figure 4.1 Gabor filtering mechanism of the human motion

4.4. Computational Neuromorphic Brain Model

The computational neuromorphic brain model consists of the visual, parietal, inferotemporal, and pre-motor cortices, along with the hypothalamus and the amygdala limbic systems. Figure 4.2 illustrates the anatomy of a human brain. A brief description about each region is as follows. The Frontal Cortex (FC) is responsible for higher cognitive functions such as judgment, motor function, attention, emotional memories, and social behavior. The Parietal Cortex (PC) is responsible for integrating sensory input coming from various parts of the body and for processing visuospatial information. The Occipital Cortex (OC) is responsible for processing visual information and is also capable of recognizing shapes and colors. The Temporal Cortex (TC) is responsible for the short-term memory of visual and auditory input. The Thalamus (TH) is responsible for processing sensory input and relaying it to the cerebral cortex. It also plays a role in regulating sleep, consciousness, and attention. The Hippocampal Formation (HF) is responsible for learning, long-term memory, and spatial navigation. The Brainstem (BS) is responsible for breathing, blood pressure, heart rate, arousal, attention, and consciousness. The Cerebellum (CB) is responsible for coordinating the movement of muscles and balance. The Corpus Callosum (CC) is responsible for interhemispheric (right and left hemispheres of the brain) communication. It also shows the dendritic release of OT into hypothalamus [22, 49, 57, 69], which is further directed to the pituitary gland. From the pituitary gland, it is discharged into various parts of the human body among which the mammary glands and uterus are of primary focus in women. The colored portions of the brain represent the parts that have been modeled.

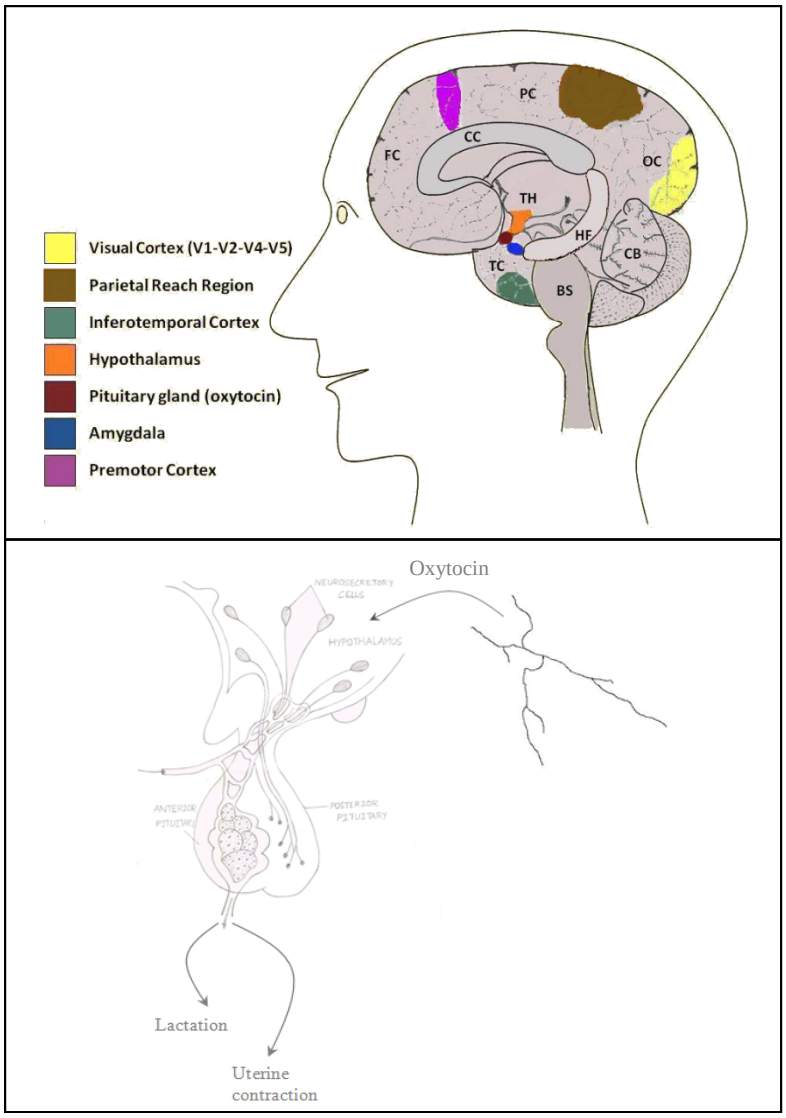

Figure 4.2 Anatomy of the human brain

In the current model the visual, parietal, and inferotemporal cortices serve as input to the hypothalamus. The visual cortex receives input from an external camera that captures human motions, the parietal cortex receives input from a VHNR based on the actions performed by it, and the inferotemporal cortex is injected a monotonic stimulus.

The RAIN network [78], which was first coined by Philip Goodman at the Brain Computation Lab, is introduced in the amygdala in order to emulate a background activity as observed in the human brain and to build a realistic brain model. There is always an on-going activity in the human brain even when the human is asleep and during the human's complete life period. The RAIN activity is the result of recurrent, asynchronous, and irregular spiking exhibited by NCS, which is analogous to the random

noise observed in an electroencephalography of the human brain [55]. A typical image of the RAIN activity is shown in Figure 4.3. There are 1300 excitatory and 300 inhibitory cells with 3% connectivity and synaptic conductances G_{exc} and G_{inh} in the RAIN network as shown in Figure 4.3A. Figure 4.3B depicts a sample RAIN activity with membrane potential shown in green and mean rate in blue. The Supra-Poissonian coefficient of variation (typically 30-50% greater than a Poisson spiking process) and the range of RAIN firing rates is between 2Hz and 60 Hz with mean rate of 14.8 Hz, which is shown in Figure 4.3C and Figure 4.3D respectively. Figure 4.3E shows the bimodal distribution of firing (n = 50 cells). Since there are many synaptic messages being sent across the RAIN network the simulation would run very slow (no closer to real-time) on a few processors. In order to run the VNR loop close to real-time with the RAIN network active we ran the simulation on a 16-processor Sun Fire X4600 cluster.

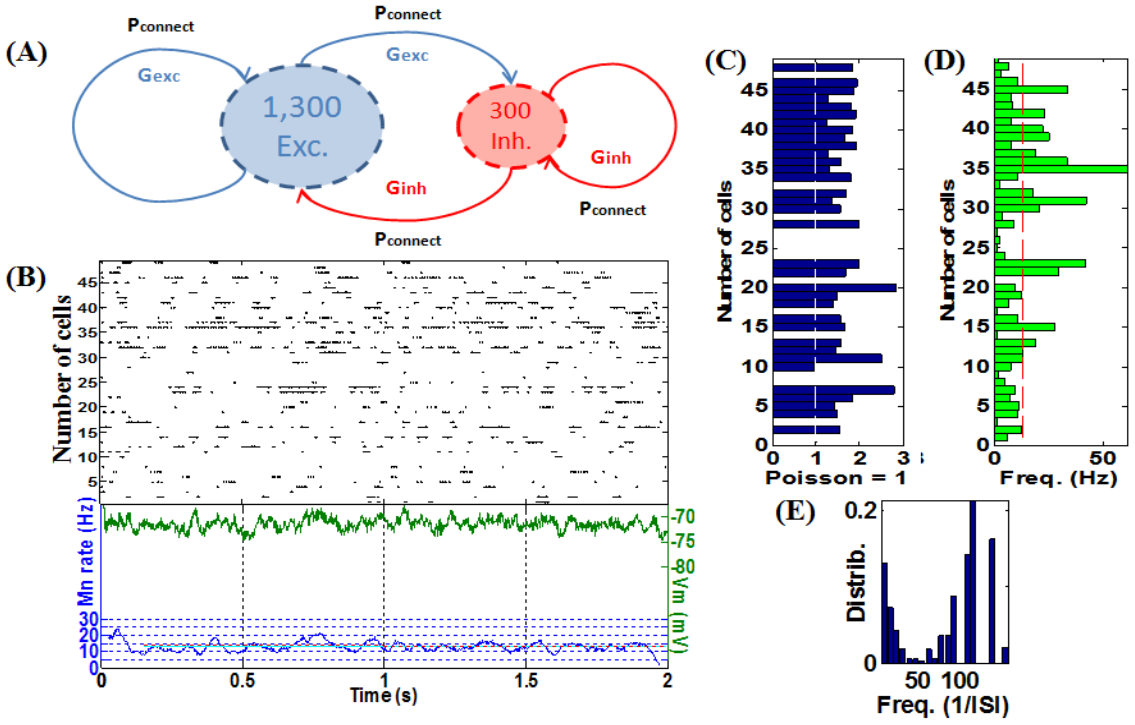

Figure 4.3 A typical RAIN activity [23]

A monotonic stimulus is injected into the parietal trust column, which is inhibited by the amygdala since there is no suppression of the amygdala activity by the hypothalamus for the discordant motion and thus distrust wins during the reach action. However, for the concordant motion, trust wins since the hypothalamus suppresses the

amygdala and there is more activity in the parietal trust column as compared to the distrust column. Based on whether the parietal trust/distrust column wins, a corresponding pre-motor column is triggered and a motor command is sent to the brainstem [63], which in turn is directed to the VHNR.

The excitatory and inhibitory connections between different parts of the computational brain model that have been simulated are shown in Figure 4.4. The computational brain model and the connections among various simulated parts of the brain are shown in Figure 4.5 for both the learning and the challenge phases.

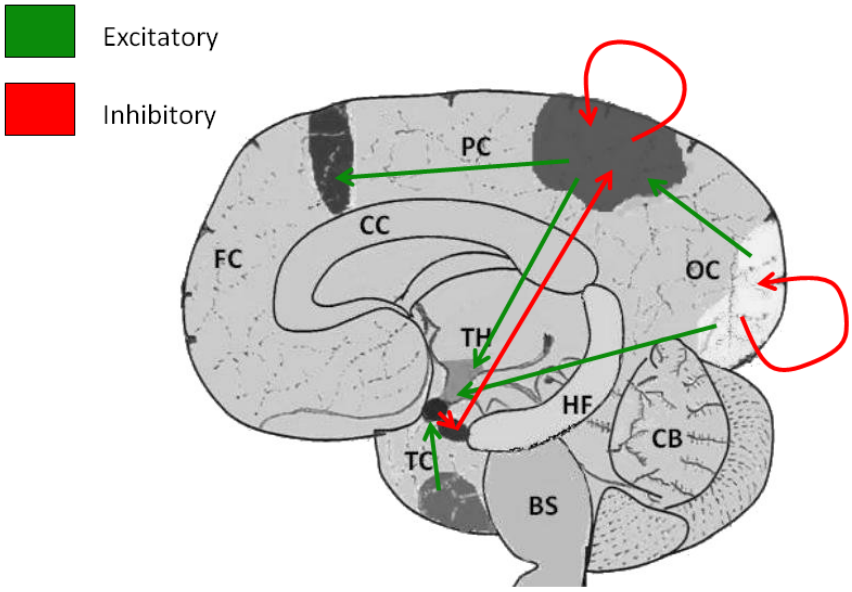

Figure 4.4 Connections within the brain

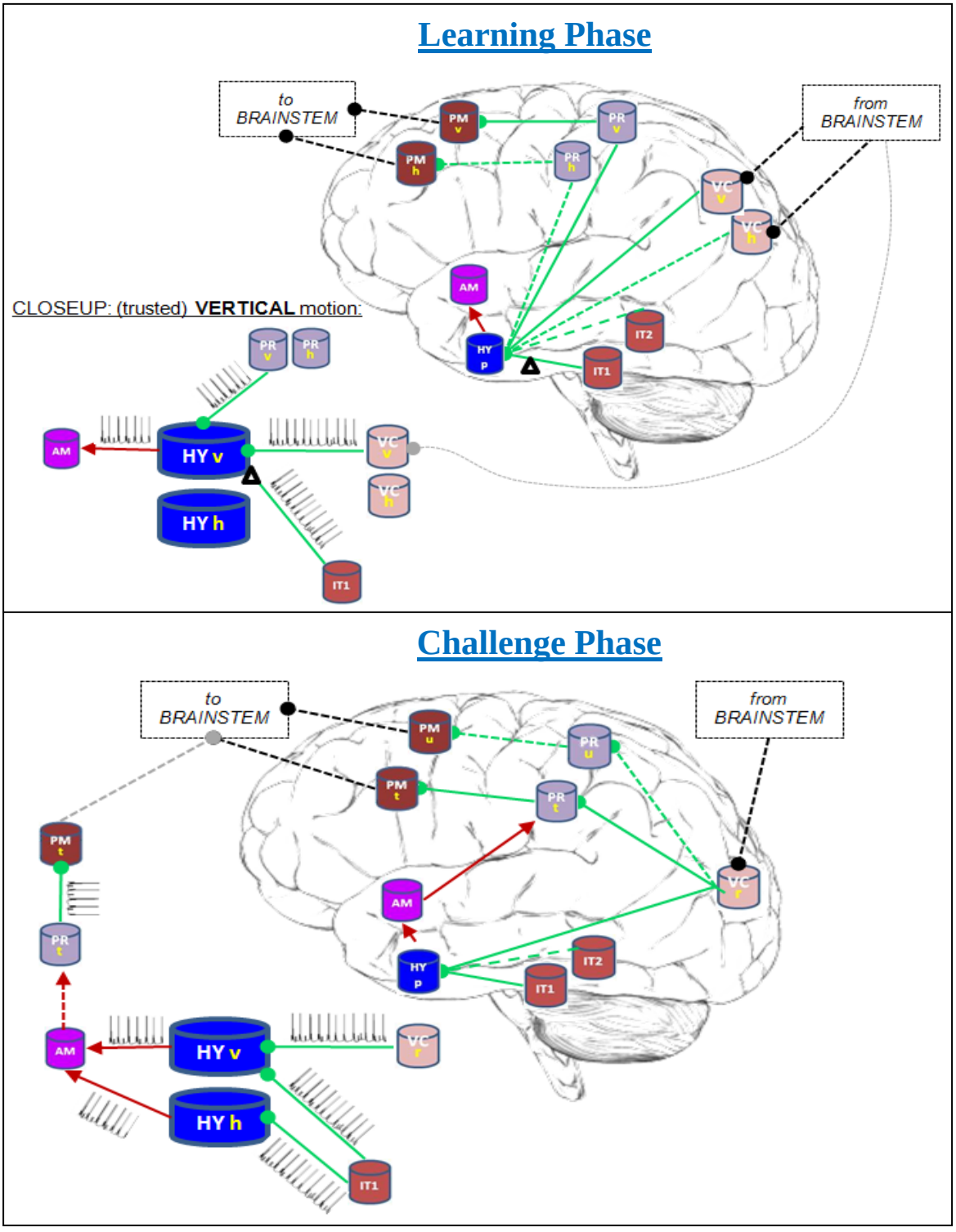

Figure 4.5 Computational brain model of the ITI architecture during the learning and challenge phases

A biologically realistic triple apical dendrite model was included in the hypothalamus. Each of the cortical columns that provide the input stimuli is connected to an independent dendrite of the hypothalamus, i.e. the visual cortex is connected to dendrite 1, the inferotemporal cortex is connected to dendrite 2, and the parietal cortex is connected to dendrite 3. Input stimuli received by the three dendrites together integrate-and-fire the hypothalamus. The dendrite connecting to the inferotemporal cortex learns to trust the human when there is sufficient firing within the hypothalamus. In this study, we used only 10 cells in each of the cortical columns except the hypothalamus, which contains 100 cells in both the vertical and horizontal columns.

4.5. Experiment Description

The robotic system consists of three layers: the robot, the NCSTools, and NCS. There is a bidirectional communication between the robot and the NCSTools, and the NCSTools and NCS as shown in Figure 4.6. The NCSTools plays the role of information relay between the robot (body) and NCS (brain) similar to that of the biological brainstem, thus making it biologically realistic. The camera sends the visual stimuli to the brain.

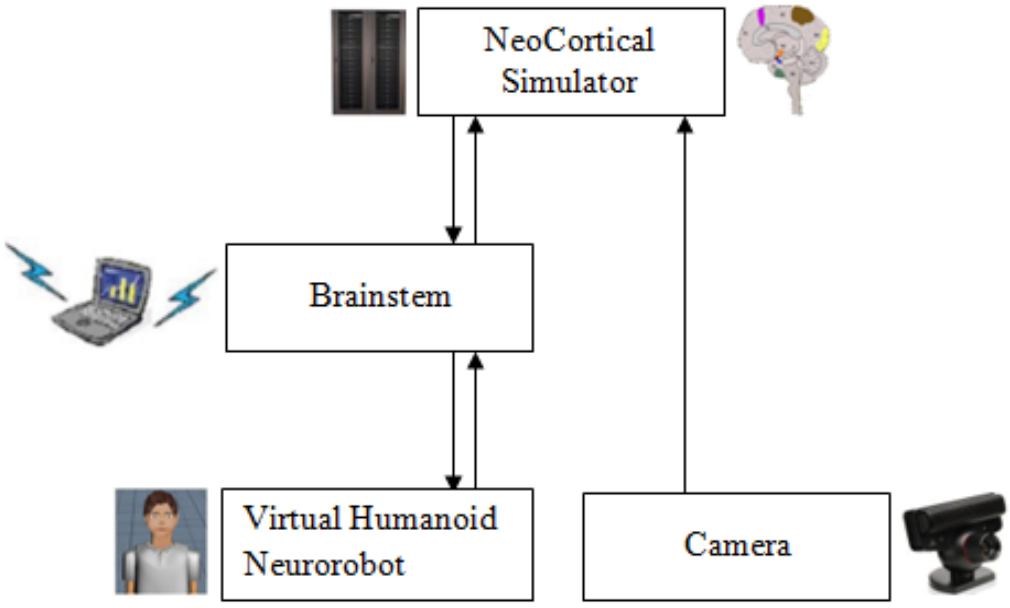

Figure 4.6 VNR loop

The input to the brain simulation and the output to the virtual neurorobotic emulator are coordinated by the NCSTools. It supports various types of input stimuli such as current, voltage, or probabilities vectors of firing, and there exists several options for output data as cell such as cell currents, voltages, spike-events, or synaptic efficacy. The parameters of the model such as long-term potentiation and depression, and spike timing dependent plasticity can be changed dynamically. It also provides a server interface to receive information from various client programs simultaneously. The flexibility to establish multiple connections aids in dynamically adding news programs to the VNR system. These programs perform various functions and the VNR system operates as a distributed neural network processing system.

It has been observed that during social interactions between two or more people, humans unconsciously and unintentionally learn to imitate the behavior of interacting partners which in turn causes an increase in affiliation between them. This is thought to be one of the reasons for group living in humans and primate species. It was proven in a biological experiment that Capuchin monkeys display affiliation towards humans who imitate them [62] and spend more time by interacting with them.

In the work presented in this thesis, the goal is to model a neuromorphic brain and implement it on a VHNR that learns to trust a human if it is being imitated by that person. On the contrary, if the VHNR is not being imitated by a human then it wouldn’t trust the person. The major parts of the human brain that need to be modeled in order for the VHNR to trust/distrust a person (corresponding to concordant or discordant actions) are the cortical columns and the limbic systems such as the visual cortex, parietal cortex, inferotemporal cortex, hypothalamus, and amygdala.

The experiment comprises learning and challenge phases which are integrated into a single setup. During the learning phase, the VHNR is programmed to perform a sequence of motions (vertical or horizontal) for 5 seconds each, for a total of 20 seconds, in the top 50% of the field of view (FOV) of the camera. The person in the real world either follows the movements of the VHNR or moves the rod perpendicular to that of the VHNR. After performing a sequence of vertical or horizontal motions for 20 seconds, if the human mimics the actions of the VHNR then the neuromorphic brain is trained sufficiently enough to trust the human, otherwise it doesn’t trust the human. During the

challenge phase, which is followed by the learning phase, if the human reaches for a dumbbell, in the bottom 50% of FOV of the camera that is placed on a table in front of him or her then a dumbbell is loaded dynamically into the virtual environment and the VHNR would preemptively hand over the dumbbell to the trusted person by happily nodding its head. On the contrary, if the person is not trusted by the VHNR then it retracts the dumbbell towards itself and shakes its head expressing anger. The experiment can be illustrated in a single statement as "Robot initiates one of two actions; then, only if the human mimics the robot's motion does *instinctive* learning-to-trust the specific face occurs, via the hypothalamic-amygdala-cortical pathway". Figure 4.7 shows the behavioral scenario.

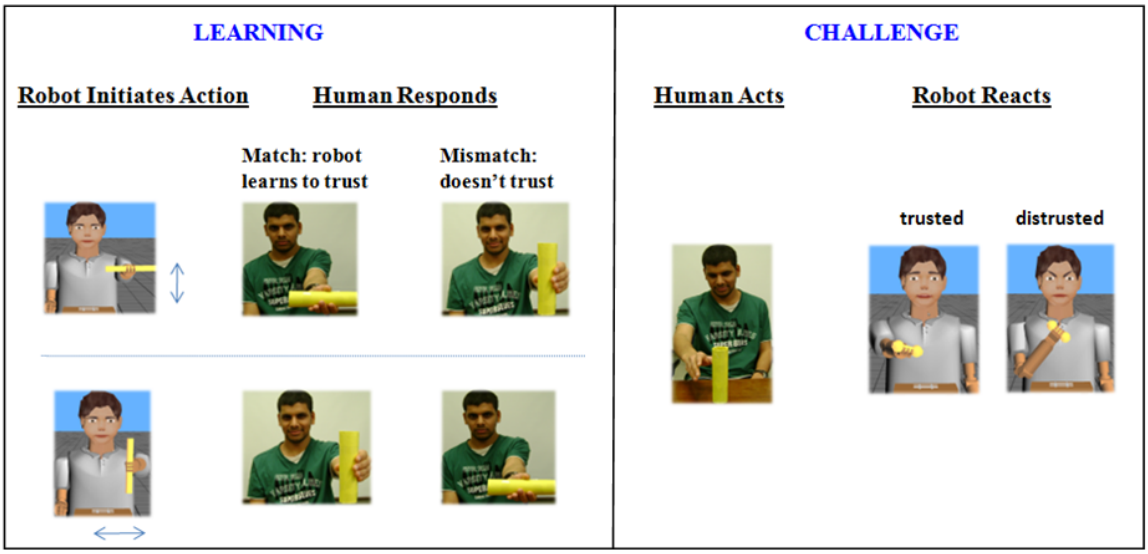

Figure 4.7 Behavioral paradigm of the ITI scenario

In this study, a VHNR is placed in front of a table in the virtual environment that holds a rod either vertically or horizontally with its left hand. This scenario is projected on a large screen. A similar setup is reflected in the real world where a person sits in front of a camera that is placed on a table and holds a rod with his or her left hand that either matches or mismatches the way a VHNR holds a rod in the virtual environment. The camera functions as a robot eye to detect the actions performed by a human such as the vertical or horizontal motions of a rod. A dumbbell is placed on the table in the real world and a similar dumbbell would be loaded into the virtual environment at a later stage of the simulation. The webots simulation of the VHNR performing vertical, horizontal,

trust, and distrust motions, and the Gabor filtering of the captured images by the camera are implemented on a desktop computer with a fairly efficient configuration (Intel Core 2 Quad, 2.40GHz, 3.00GB RAM). The simulation of the brain dynamics using the NCS and the signaling of a motor command to the VHNR by the brainstem, corresponding to the firing rates of motor cells, are implemented on the *cortex2* cluster (48-processor Sun Fire X4600).

Chapter 5: Results

In this chapter, we demonstrate several results of the study presented in this thesis. The results are organized as the concordant and discordant robot-human motions, the Gabor screenshots, and demonstration of the ITI scenario. Concordant and discordant robot-human motions discuss firing patterns in the cortical columns, response of the hypothalamus to the cortical stimuli, the amygdala RAIN activity in response to the hypothalamic firing, the synaptic weight distributions, the firing patterns in the parietal decision-making cortical columns, and the dendritic spiking within the hypothalamus. All the results presented in Sections 5.1 and 5.2 show the firing rates of a single cell except for the RAIN activity, which shows the firing rates of all the cells.

5.1. Concordant Robot-Human Motion

Firing Patterns in the Cortical Columns

The firing patterns in the visual, parietal, and inferotemporal cortices are discussed below. The visual cortex responds to the human motion, since the camera sends stimuli to the visual cortex based on the actions performed by a human. The parietal cortex responds to the robot motion, since stimuli are sent to the parietal cortex based on the actions performed by a robot. The inferotemporal cortex is injected a monotonic stimulus for the whole simulation period.

Inferotemporal Cortex

Figure 5.1 shows a monotonic stimulus injected into the inferotemporal cortex for the complete simulation time, which is of 40 seconds. The same monotonic stimulus is injected into the inferotemporal cortex during the discordant motion as well. The inferotemporal cortex learns to recognize a trusted person by strengthening the synaptic USE value of the synapses connecting to the hypothalamus.

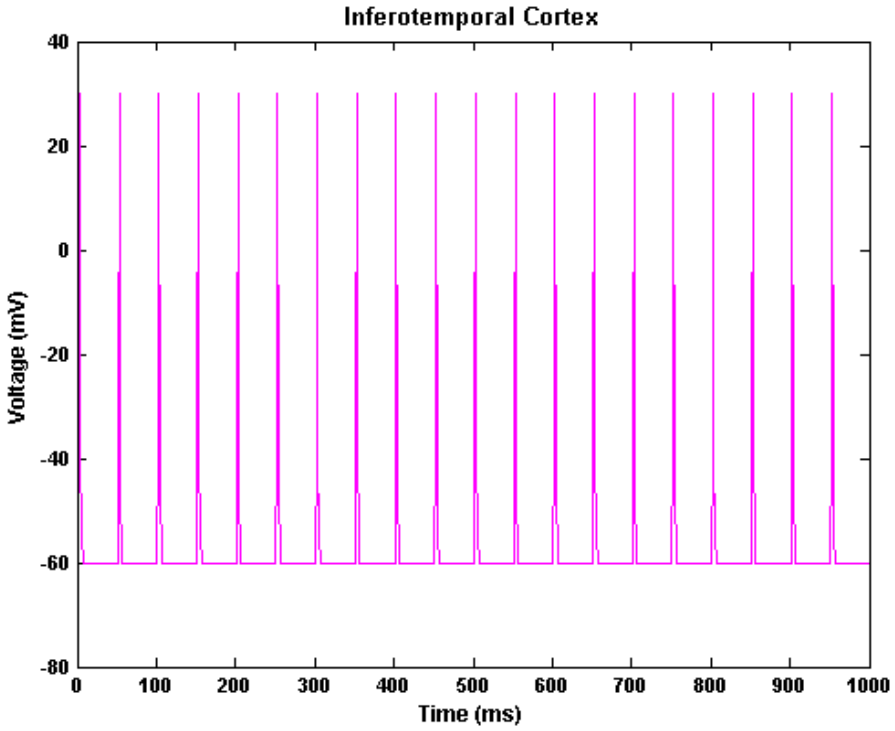

Figure 5.1 Consistent firing patterns observed in the inferotemporal cortex during both the concordant and discordant motions

Visual Cortex

Figures 5.2 and 5.3 show the firing patterns in the vertical and horizontal columns of the visual cortex for the whole simulation period, which is of 40 seconds. Each set of vertical and horizontal motions is performed for 5 seconds (alternatively) starting with the vertical motion. The human performs the vertical and horizontal motions for a total of 25 seconds as observed in the visual cortex. From these figures it can be seen that when the membrane potential of a cell reaches its threshold, spike firing occurs and causes each spike to reach 30 mV.

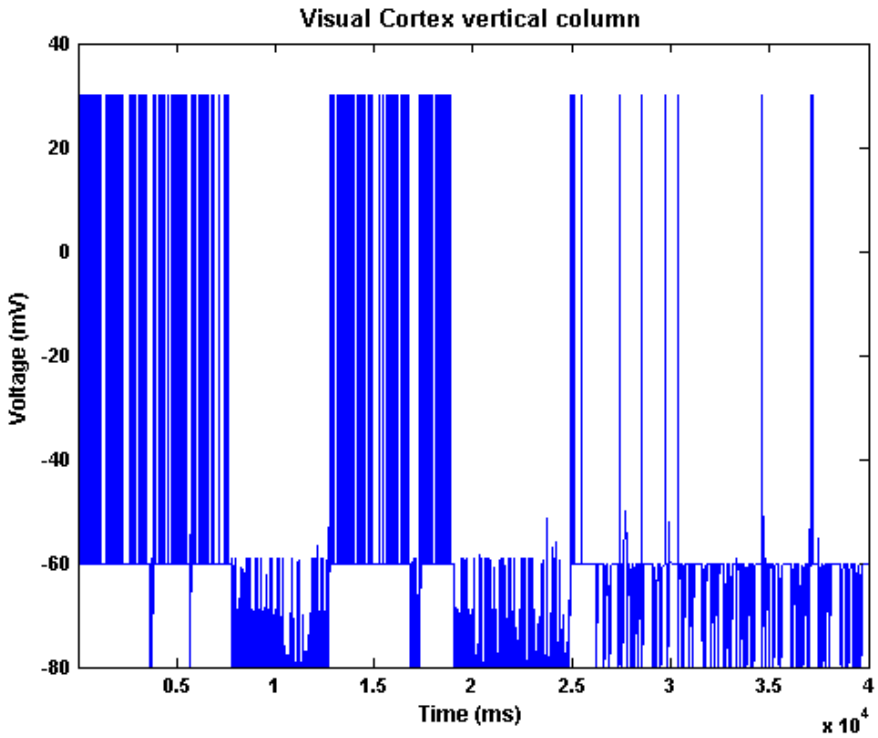

Figure 5.2 Firing patterns observed in the vertical column of the visual cortex during the concordant motion

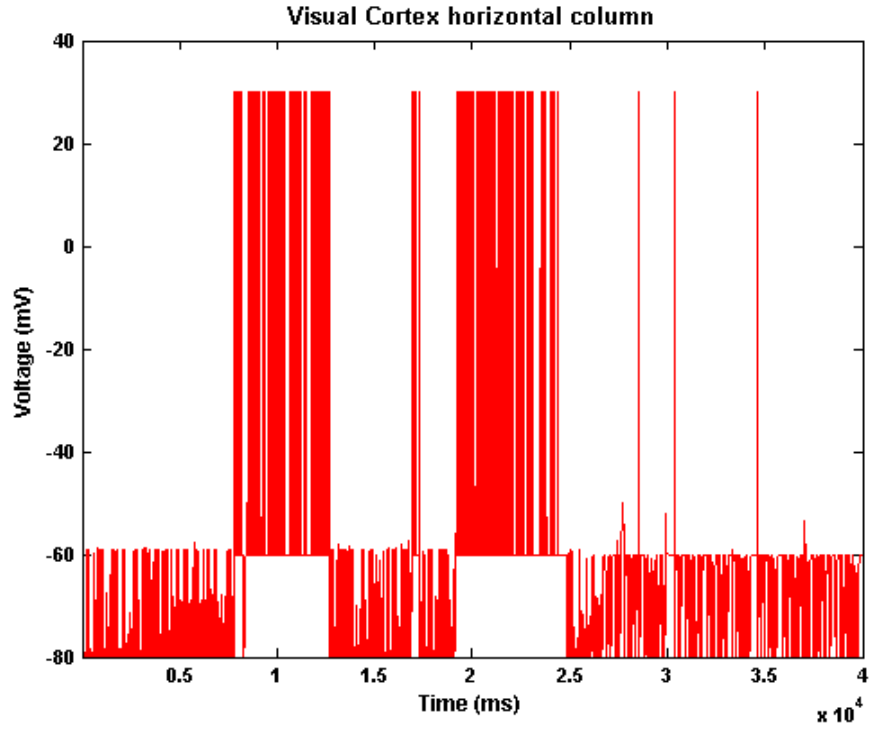

Figure 5.3 Firing patterns observed in the horizontal column of the visual cortex during the concordant motion

Parietal Cortex

Figures 5.4 and 5.5 show the firing patterns in the vertical and horizontal columns of the parietal cortex for the whole simulation period, which is of 40 seconds. Similar to the activity in the visual cortex, the parietal cortex shows the firing patterns of stimuli from the vertical and horizontal motions, each of which is performed for 5 seconds (alternatively) starting with the vertical motion. Also, firing of each spike reaches 30 mV.

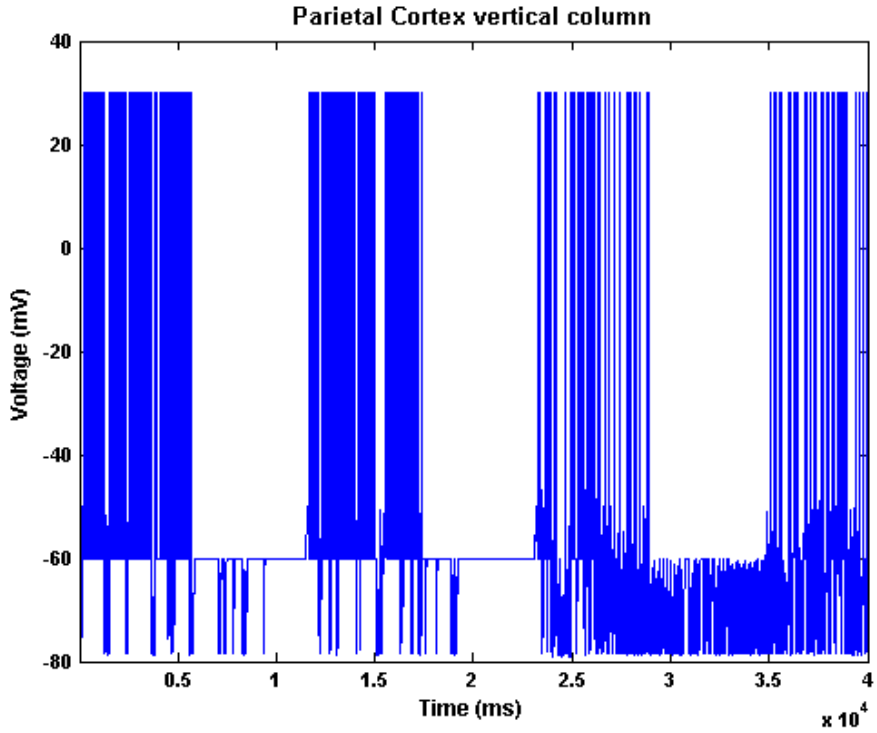

Figure 5.4 Firing patterns observed in the vertical column of the parietal cortex during the concordant motion

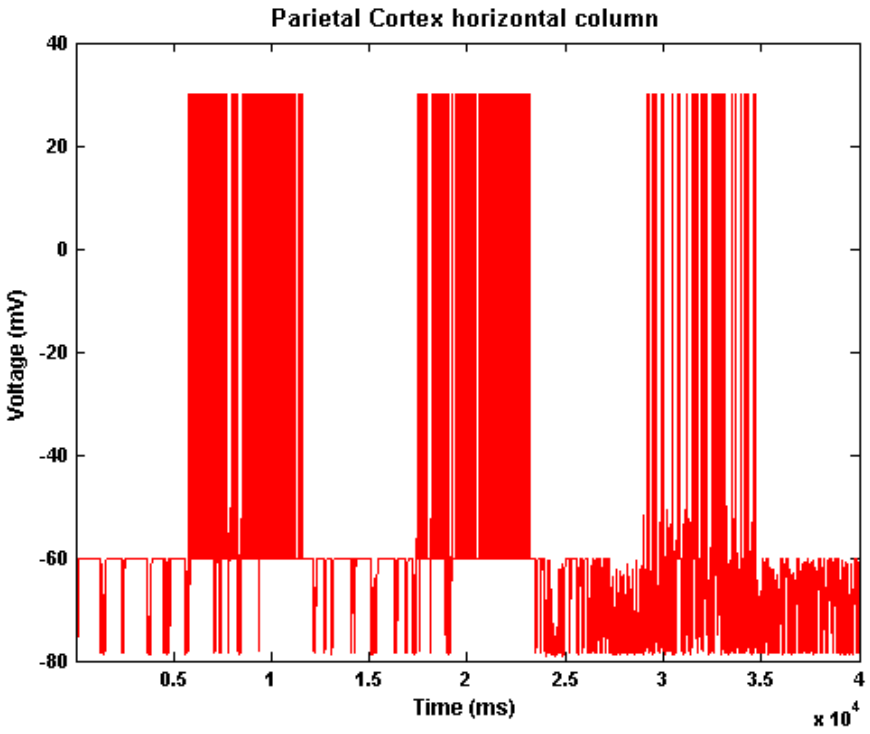

Figure 5.5 Firing patterns observed in the horizontal column of the parietal cortex during the concordant motion

Hypothalamic Response to the Cortical Stimuli

Figures 5.6 and 5.7 show the significant firing patterns observed in the vertical and horizontal columns of the hypothalamus over a period of 40 seconds. The hypothalamic firing is a result of the overlap in the spiking activities of visual, parietal, and inferotemporal cortices.

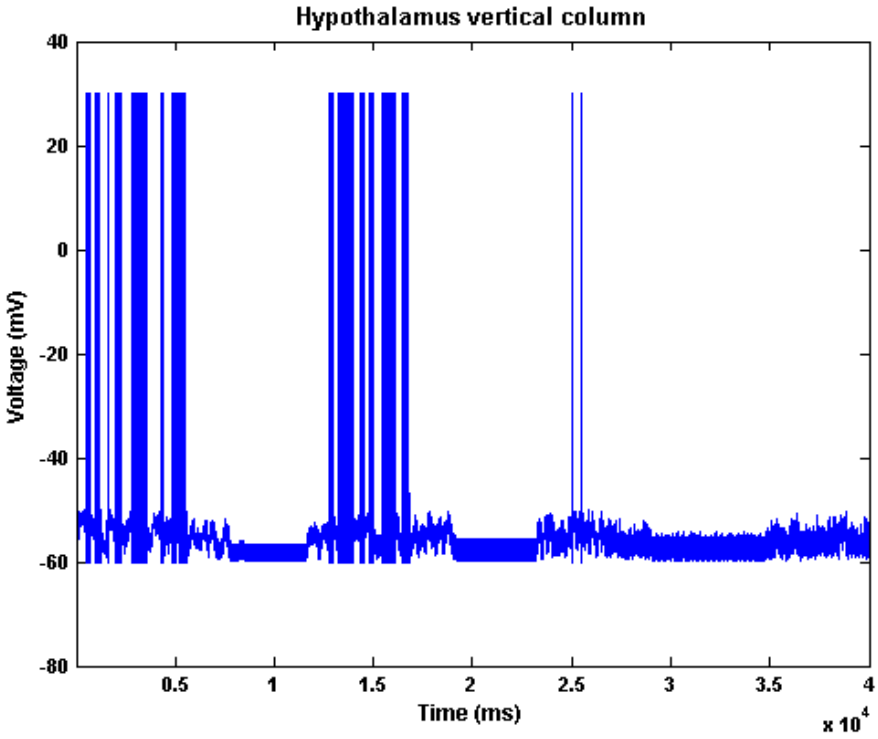

Figure 5.6 Firing patterns observed in the vertical column of the hypothalamus in response to the cortical stimuli during the concordant motion

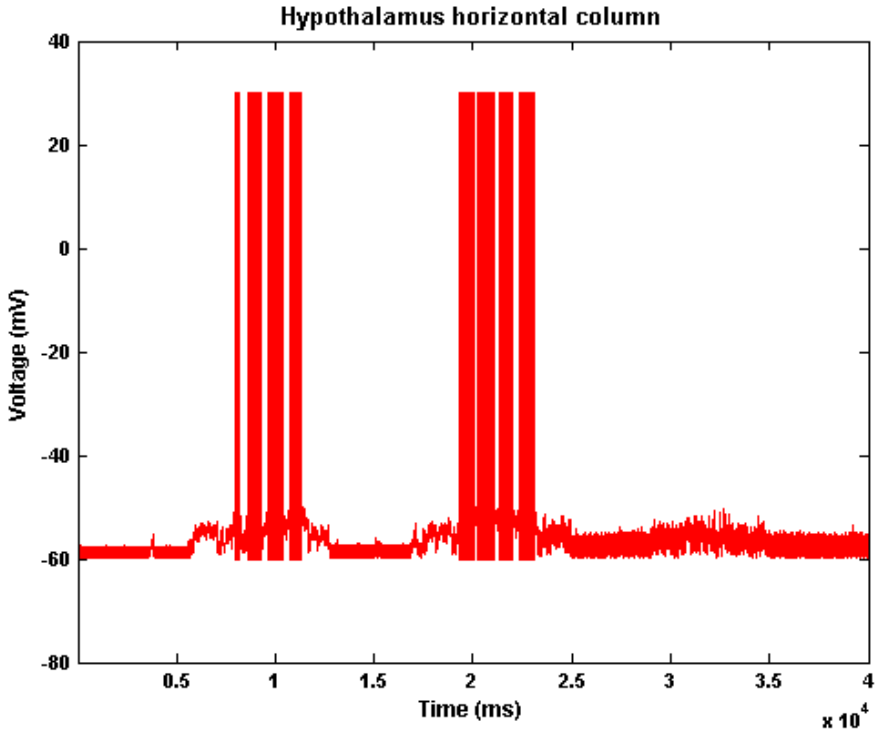

Figure 5.7 Firing patterns observed in the horizontal column of the hypothalamus in response to the cortical stimuli during the concordant motion

Amygdala RAIN Network

Figure 5.8 shows the RAIN activity in the amygdala that was shut down by the hypothalamic firing after sufficient learning to trust a person has occurred.

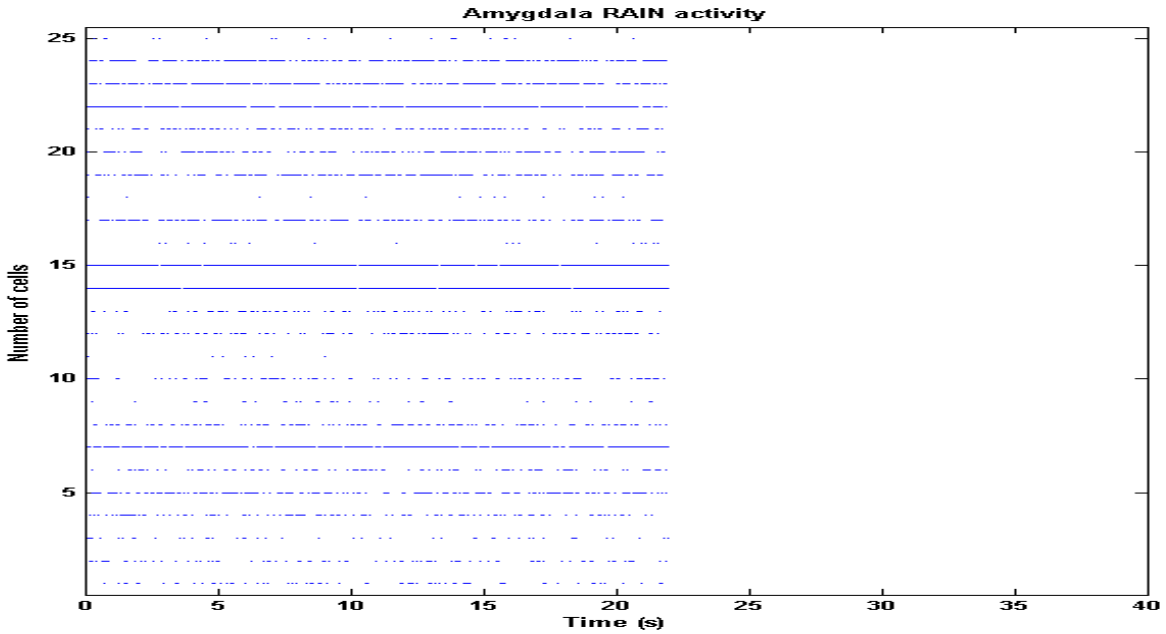

Figure 5.8 Suppression of the RAIN activity by the hypothalamus observed in the amygdala during the concordant motion

Synaptic Weight Distributions

Figures 5.9 and 5.10 show the synaptic weight distributions of synapses connecting from the vertical and horizontal columns of the inferotemporal cortex to the hypothalamus. It is observed that there is a significant rise in the synapse USE value during the concordant motion.

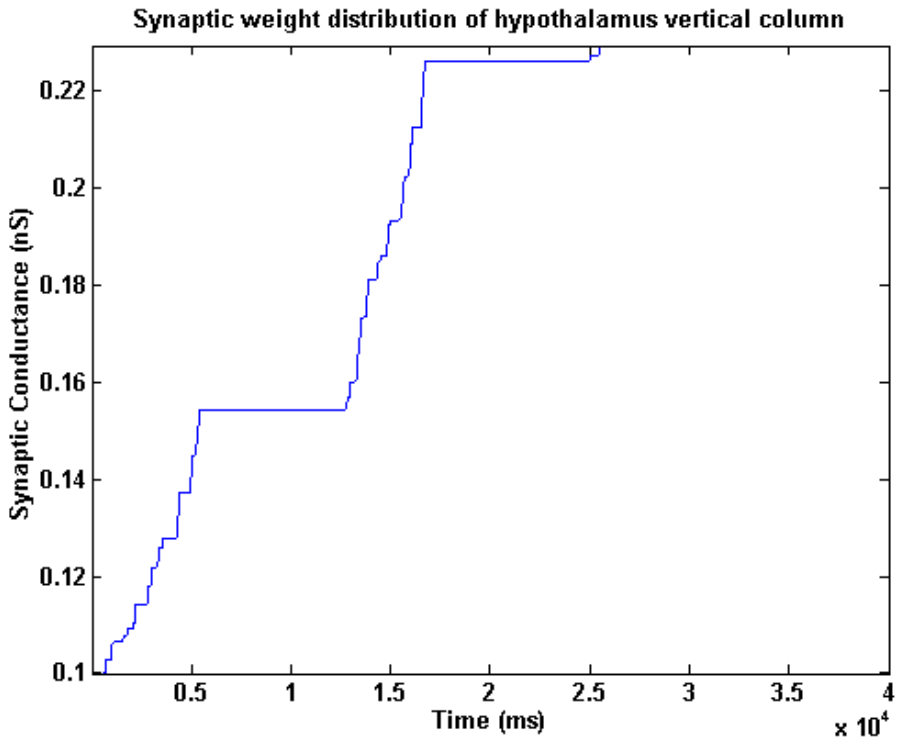

Figure 5.9 Rate of increase of the synaptic USE value corresponding to the vertical column of the hypothalamus during the concordant motion

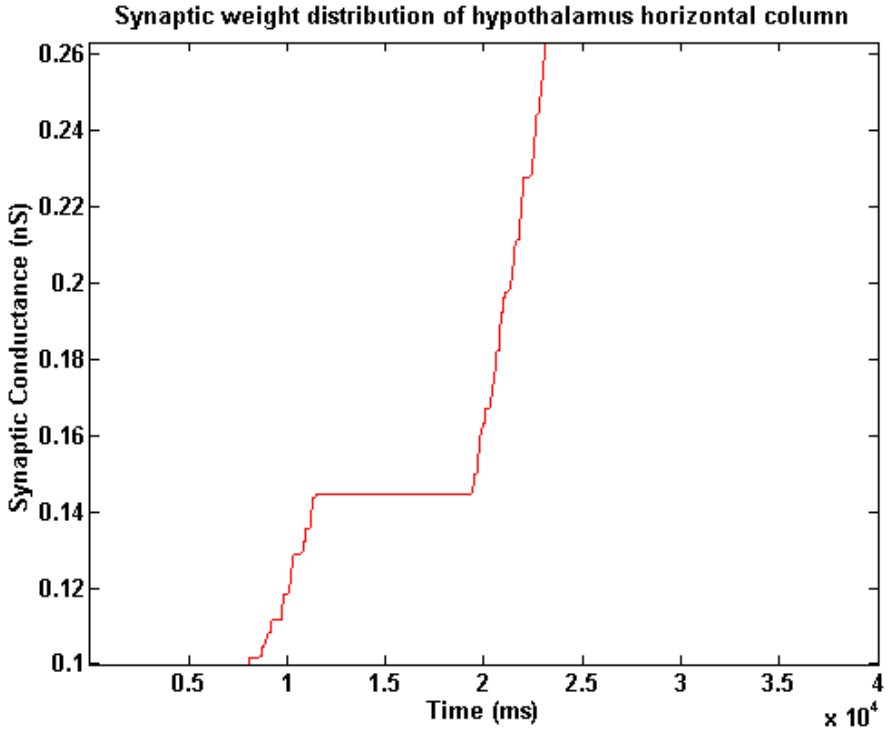

Figure 5.10 Rate of increase of the synaptic USE value corresponding to the horizontal column of the hypothalamus during the concordant motion

Activity in the Parietal Decision-Making Cortical Columns

Figure 5.11 shows the activity in the reach column of the visual cortex over a period of 40 seconds due to the human reach motion. It is observed that reaching for an object is performed at 25 seconds. During the reach motion, a relatively significant firing occurs in only one of the parietal decision-making cortical columns corresponding to the concordant or discordant robot-human motions to decide upon a single winner. Figures 5.12 and 5.13 show the firing patterns in the parietal trust and distrust columns. It can be seen that the firing in the trust column is relatively high as compared to the distrust column. The reason is that because of a shut down in the amygdala RAIN activity there is an insufficient inhibition of the trust column and thus it fires more.

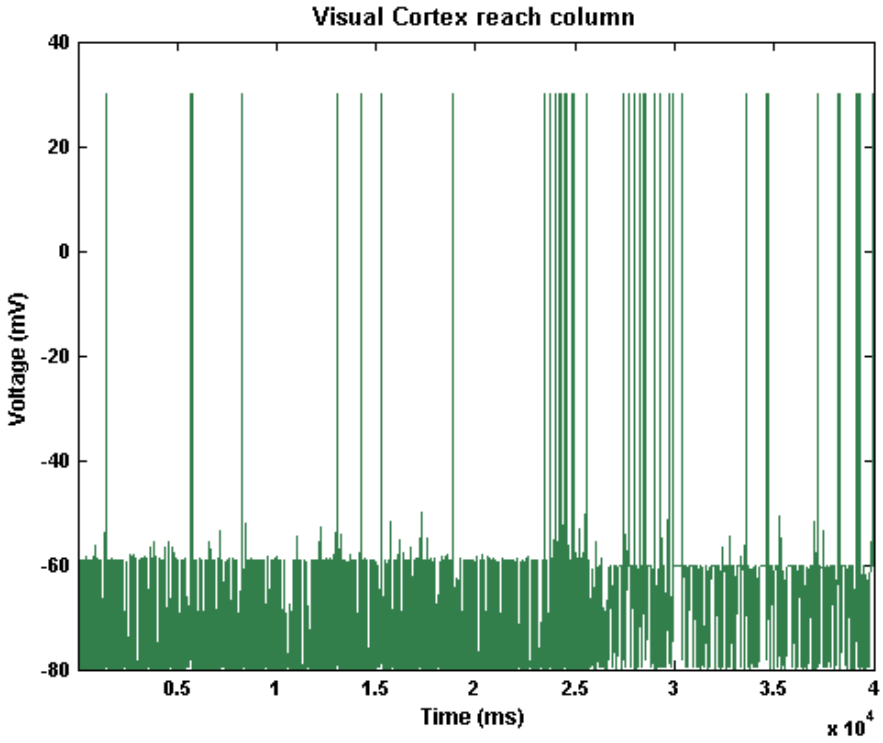

Figure 5.11 Spiking activity observed in the reach column of the visual cortex due to the human reach action during the concordant motion

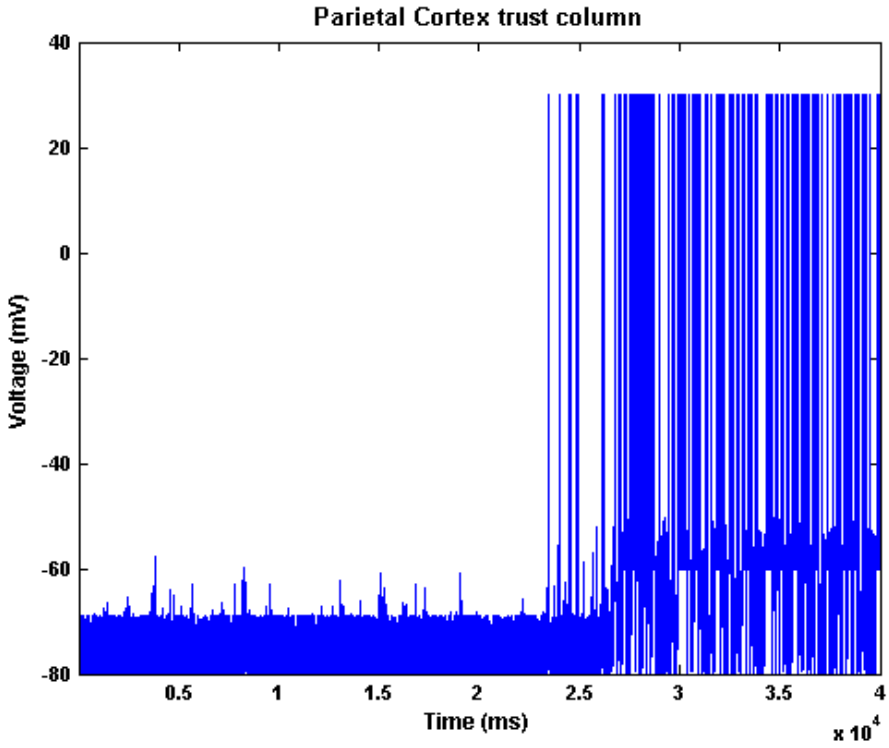

Figure 5.12 Significant spiking activity observed in the trust column of the parietal cortex during the human reach action for the concordant motion

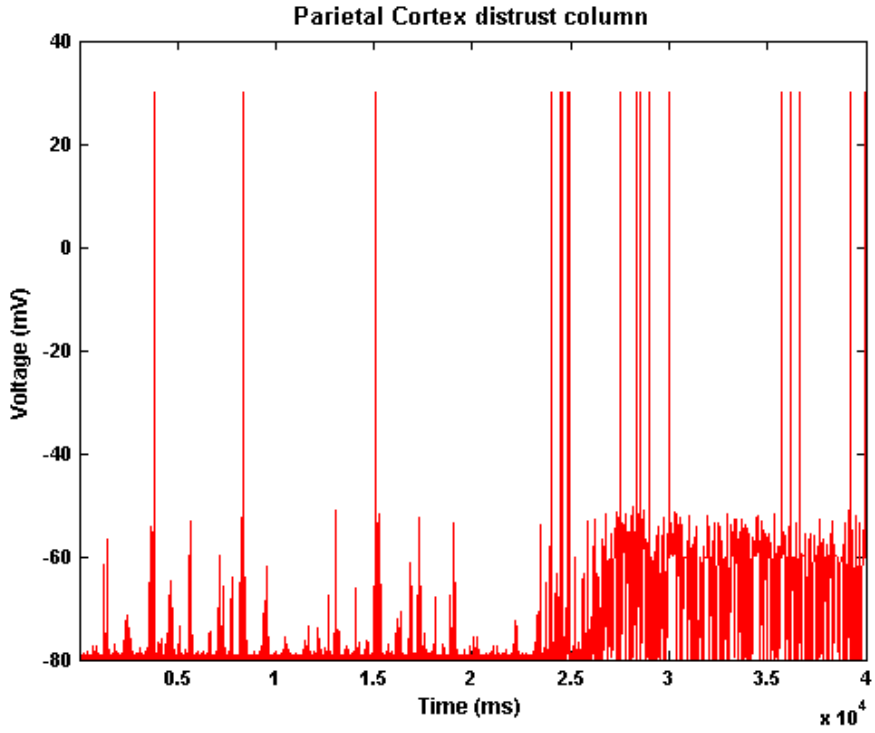

Figure 5.13 Less spiking activity observed in the distrust column of the parietal cortex during the human reach action for the concordant motion

Dendritic Spiking within the Hypothalamus

The visual, parietal, and inferotemporal cortices are connected to the independent dendrites of the hypothalamus and the firing in the hypothalamus occurs only when the stimuli from all three dendrites integrate and fire together. Figure 5.14 shows the spiking in the independent dendrites of the hypothalamus. It is observed that there is a high spiking in the dendrite connecting to the inferotemporal cortex. The reason is that for a significant amount of firing within the hypothalamus a synapse connecting from the inferotemporal cortex to the hypothalamus gets strengthened.

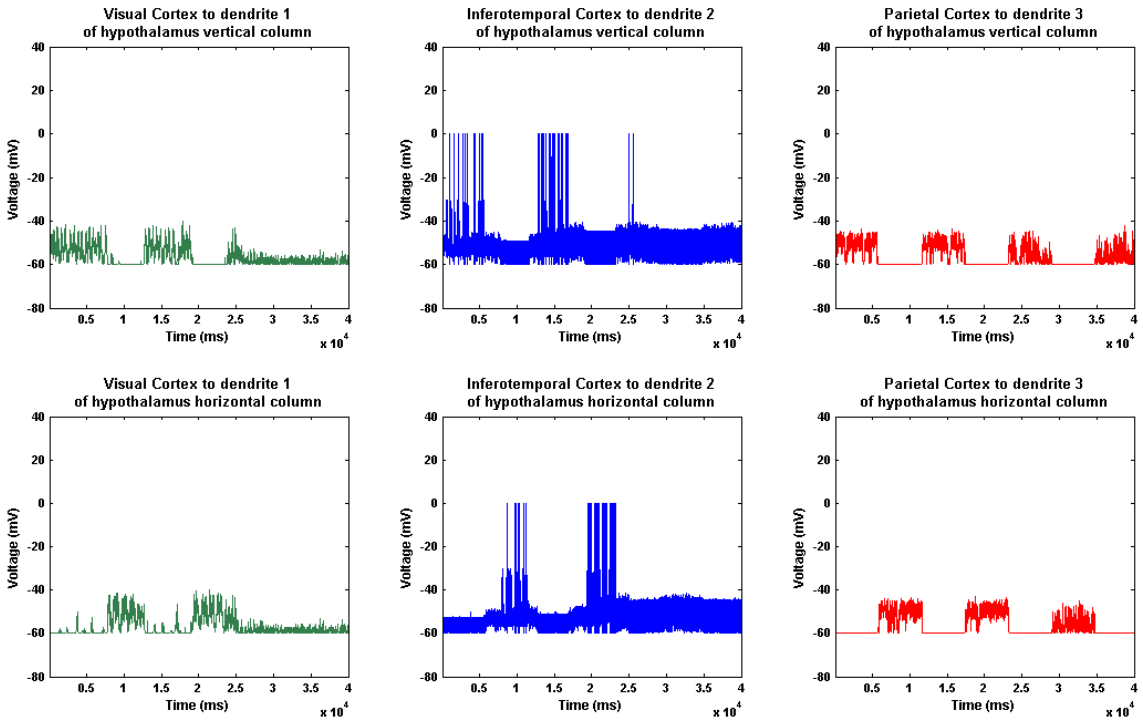

Figure 5.14 Spiking patterns observed within the individual dendrites of the hypothalamus during the concordant motion

5.2. Discordant Robot-Human Motion

Firing Patterns in the Cortical Columns

The firing patterns in the visual, parietal, and inferotemporal cortices for the discordant motion are discussed below.

Inferotemporal Cortex

As mentioned above, the activity in the inferotemporal cortex is identical for both the concordant and discordant motions.

Visual Cortex

Figures 5.15 and 5.16 show the firing patterns in the vertical and horizontal columns of the visual cortex for the whole simulation period, which is of 40 seconds. The activity is similar to that of the concordant motion with respect to three things: performing each set of vertical and horizontal motions for 5 seconds, the firing of spikes to a threshold of 30 mV, and alternating between vertical and horizontal motions. The only difference is that during the discordant motion the sequence of actions is initiated with the horizontal motion. There is a significant activity observed in the visual cortex for a total of 25 seconds.

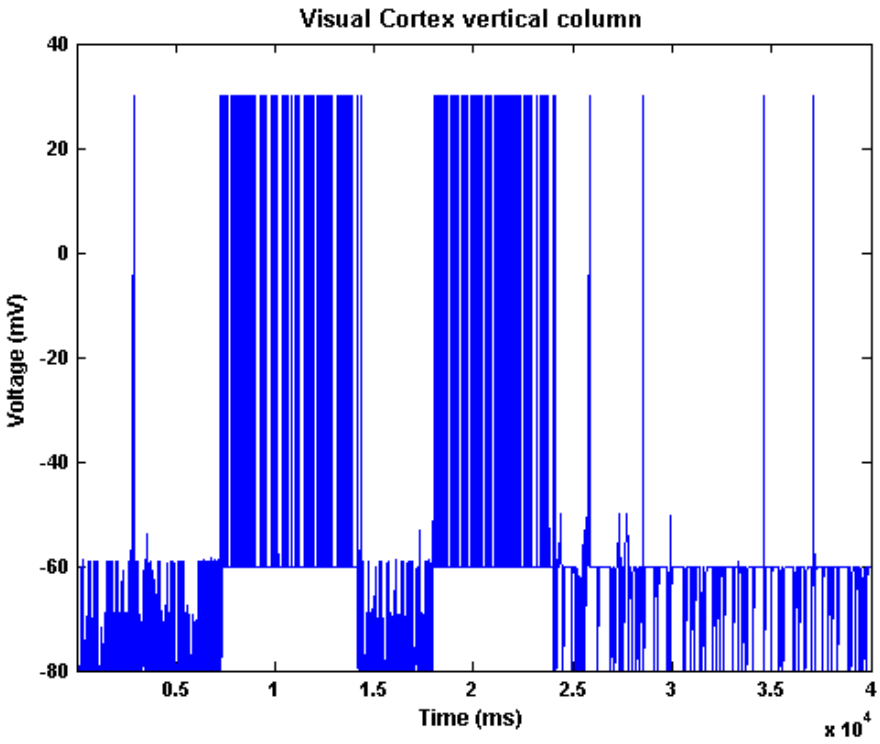

Figure 5.15 Firing patterns observed in the vertical column of the visual cortex during the discordant motion

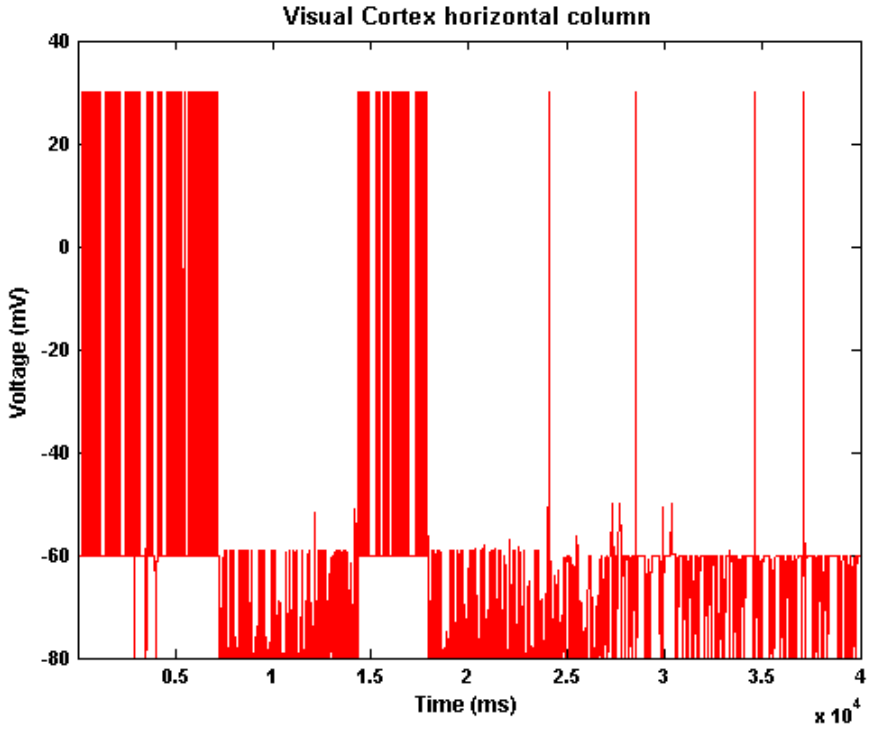

Figure 5.16 Firing patterns observed in the horizontal column of the visual cortex during the discordant motion

Parietal Cortex

Figures 5.17 and 5.18 show the firing patterns in the vertical and horizontal columns of the parietal cortex for the whole simulation period, which is of 40 seconds.

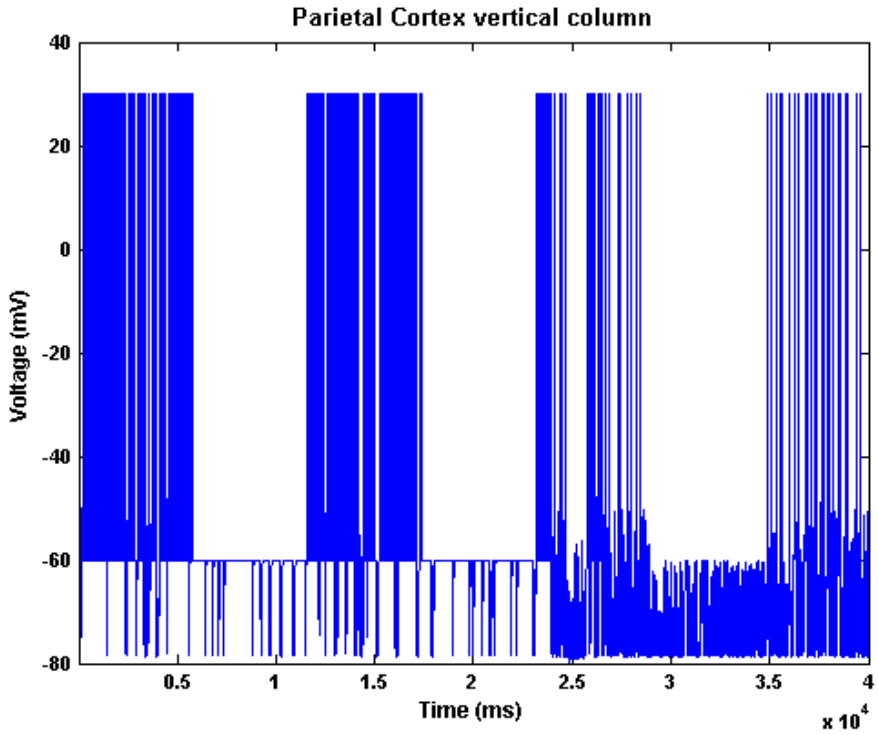

Figure 5.17 Firing patterns observed in the vertical column of the parietal cortex during the discordant motion

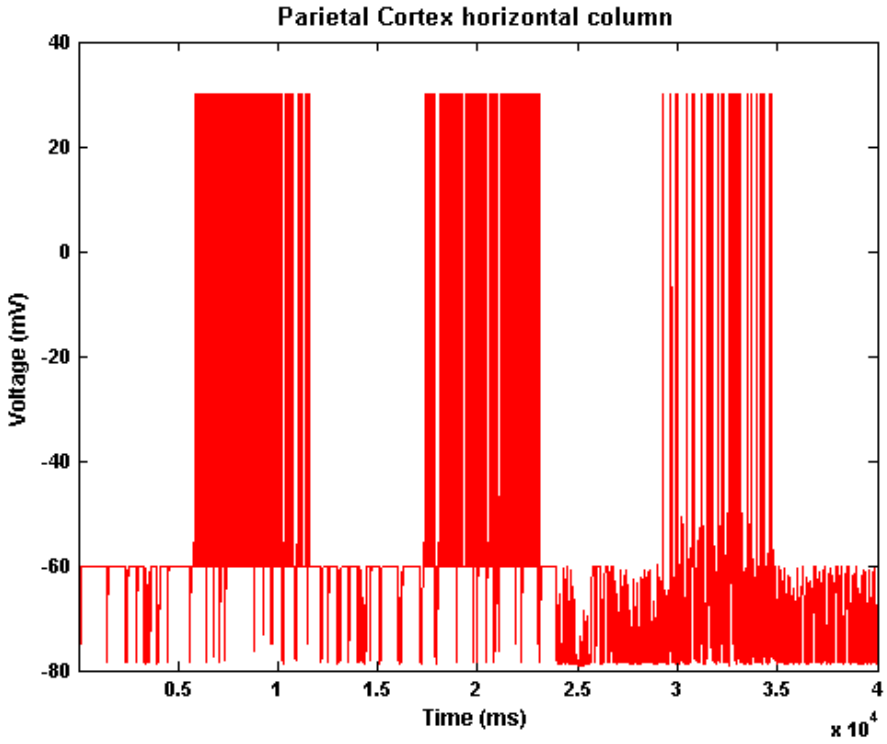

Figure 5.18 Firing patterns observed in the horizontal column of the parietal cortex during the discordant motion

Hypothalamic Response to the Cortical Stimuli

Figures 5.19 and 5.20 show the insignificant firing patterns observed in the vertical and horizontal columns of the hypothalamus over a period of 40 seconds. Since there is very little overlap in the spiking activities of visual, parietal, and inferotemporal cortices no considerable firing is observed in the hypothalamus.

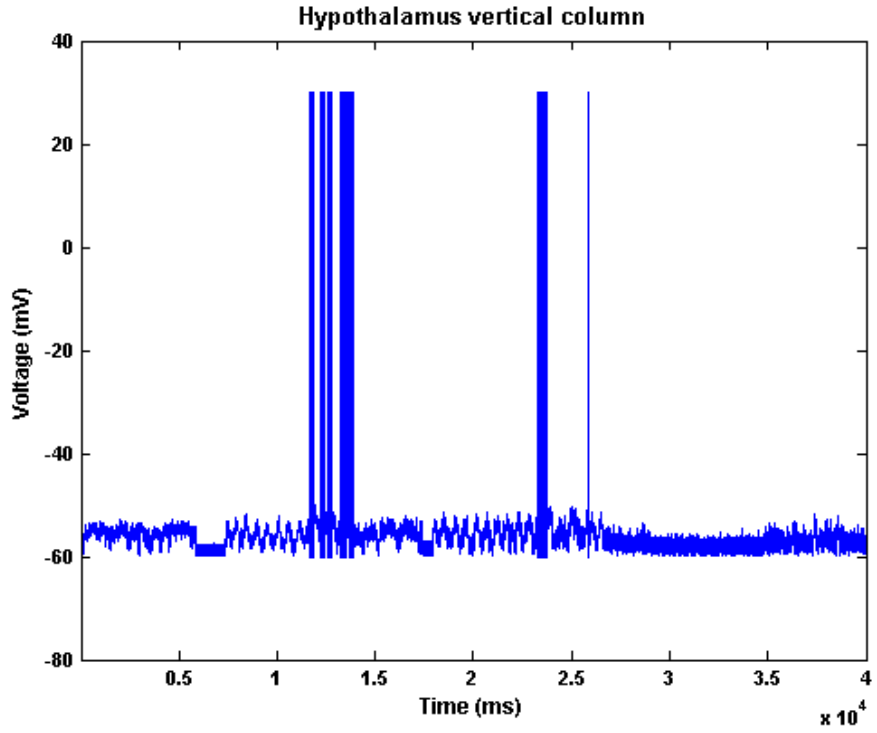

Figure 5.19 Firing patterns observed in the vertical column of the hypothalamus in response to the cortical stimuli during the discordant motion

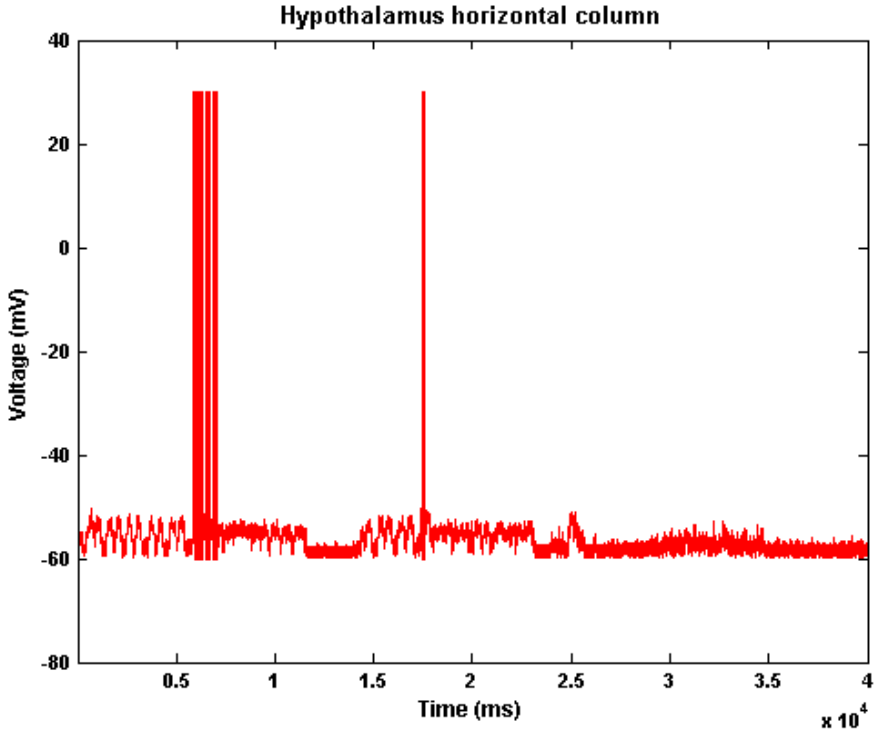

Figure 5.20 Firing patterns observed in the horizontal column of the hypothalamus in response to the cortical stimuli during the discordant motion

Amygdala RAIN Network

Figure 5.21 shows the complete RAIN activity in the amygdala. Since the hypothalamic firing is low during the discordant motion, it cannot suppress the RAIN activity present in the amygdala.

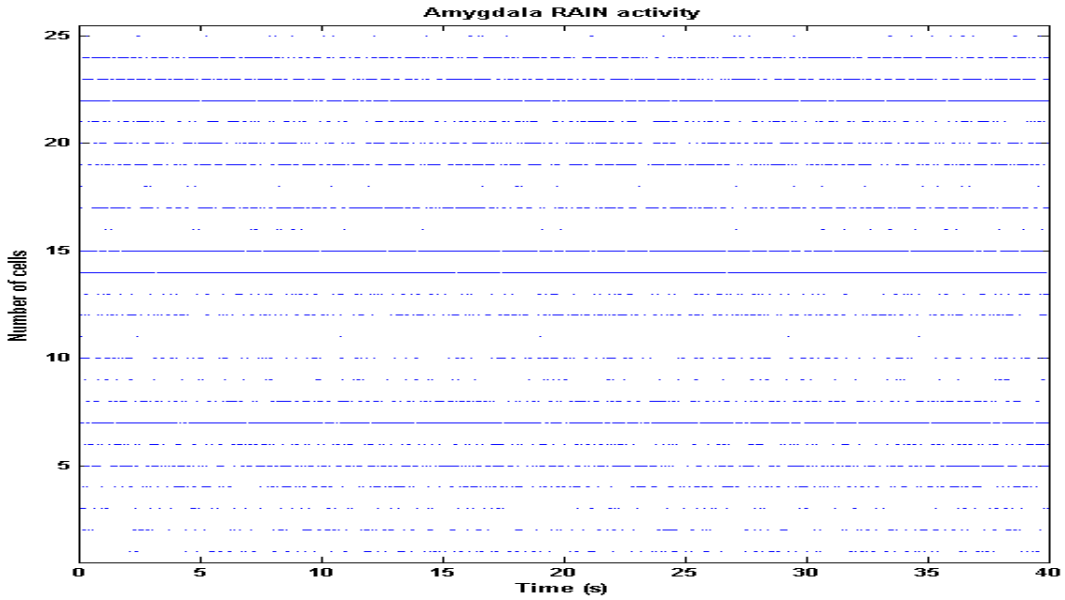

Figure 5.21 Complete RAIN activity observed in the amygdala during the discordant motion

Synaptic Weight Distributions

Figures 5.22 and 5.23 show the synaptic weight distributions of the synapses connecting from the vertical and horizontal columns of the inferotemporal cortex to the hypothalamus. It is observed that there is a very little rise in the synapse USE value as compared to the concordant motion.

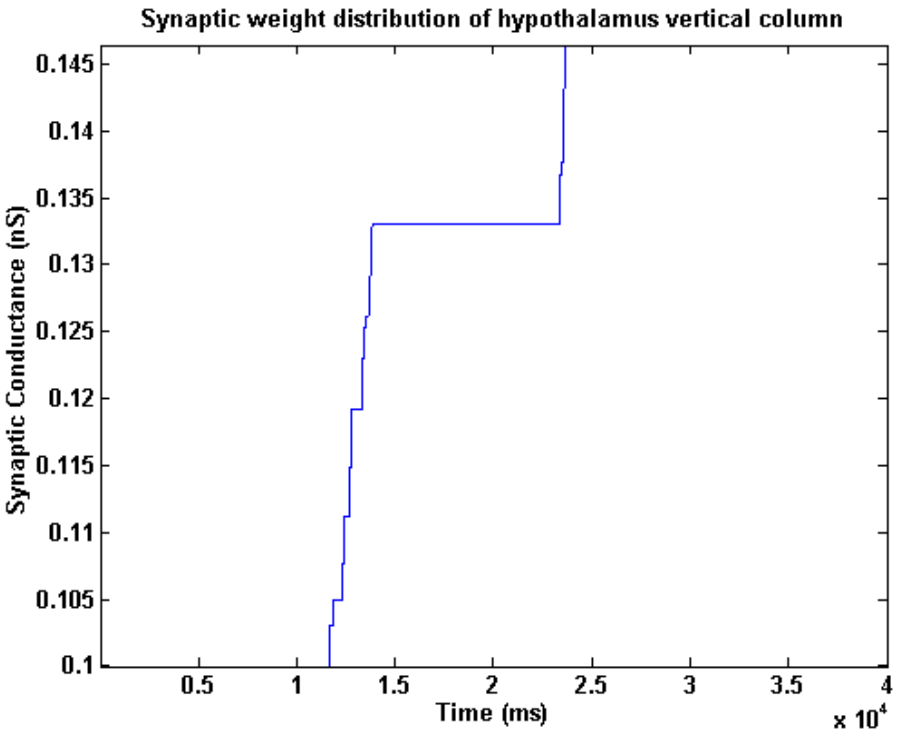

Figure 5.22 Rate of increase of the synaptic USE value corresponding to the vertical column of the hypothalamus during the discordant motion

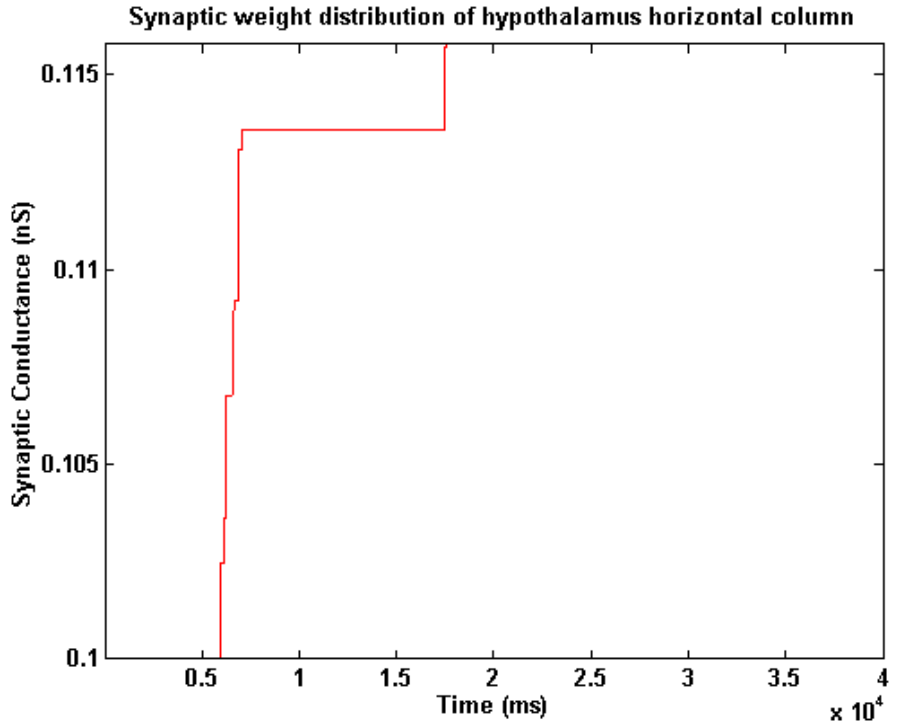

Figure 5.23 Rate of increase of the synaptic USE value corresponding to the horizontal column of the hypothalamus during the discordant motion

Activity in the Parietal Decision-Making Cortical Columns

Figure 5.24 shows the activity in the reach column of the visual cortex over a period of 40 seconds due to the human reach motion. Figures 5.25 and 5.26 show the firing patterns observed in the parietal trust and distrust columns and it can be seen that the firing in the distrust column is relatively high as compared to the trust column. The reason is the RAIN activity present in the amygdala inhibits the activity in the trust column.

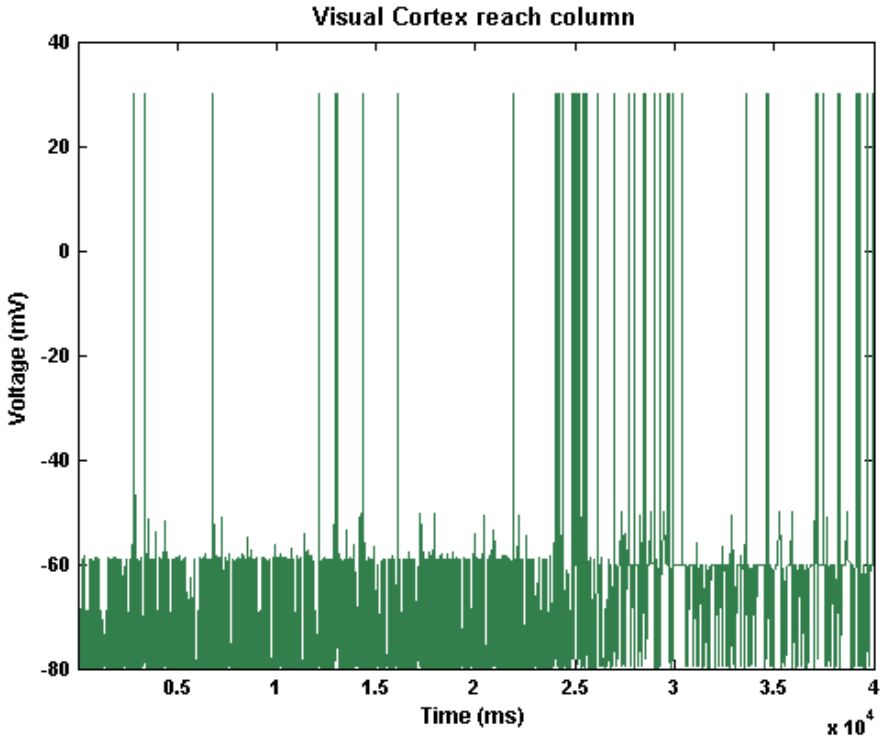

Figure 5.24 Spiking activity observed in the reach column of the visual cortex due to the human reach action during the discordant motion

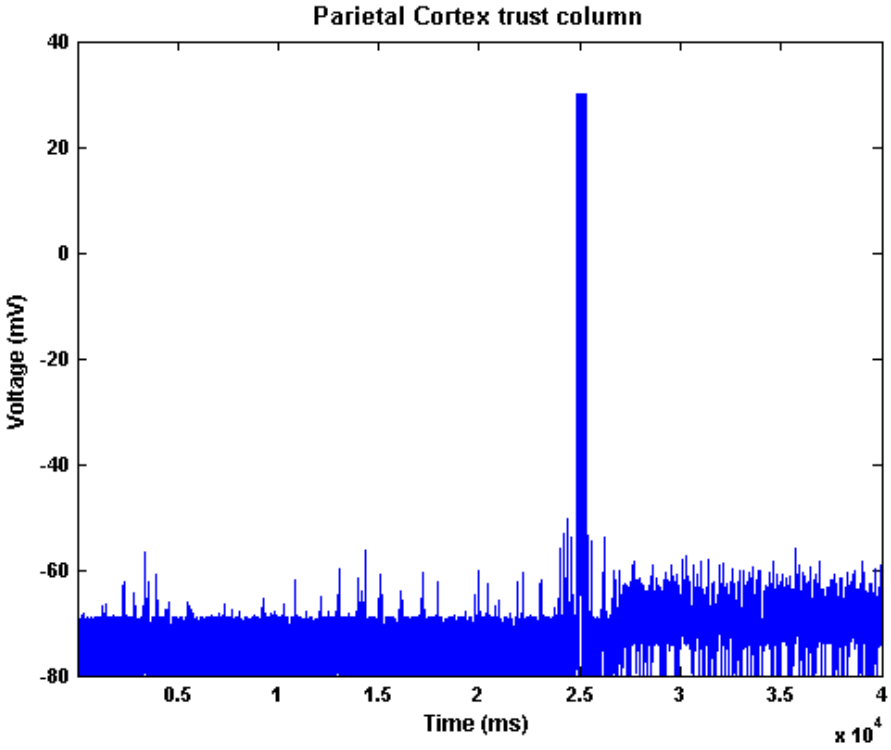

Figure 5.25 Less spiking activity observed in the trust column of the parietal cortex during the human reach action for the discordant motion

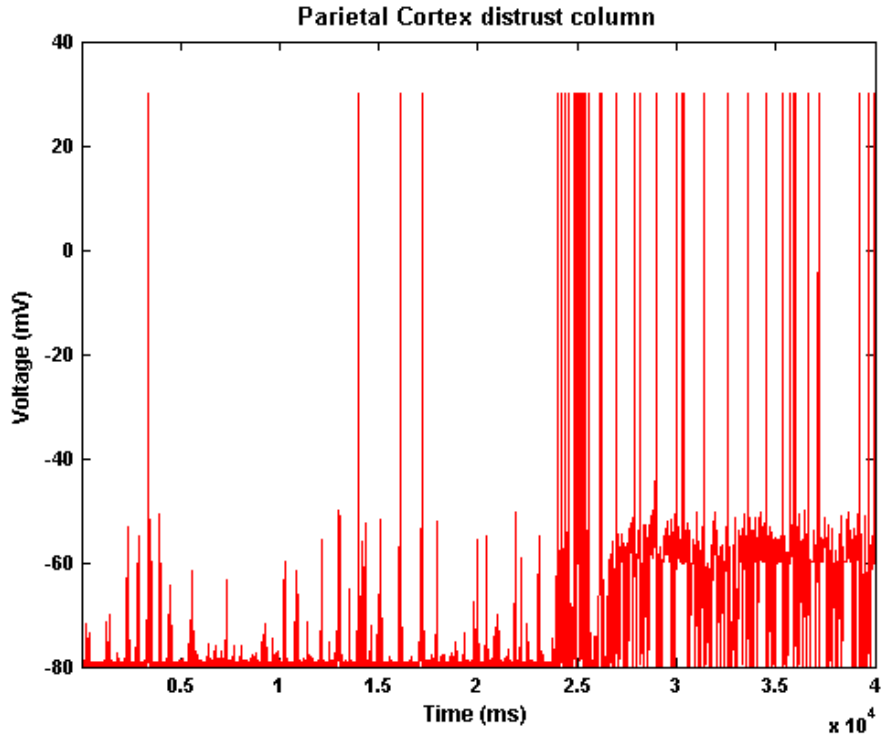

Figure 5.26 Significant spiking activity observed in the distrust column of the parietal cortex during the human reach action for the discordant motion

Dendritic Spiking within the Hypothalamus

Figure 5.27 shows the spiking in the independent dendrites of the hypothalamus. It is observed that there is a low spiking activity in the dendrite connecting to the inferotemporal cortex, which is obvious due to lack of the hypothalamic firing.

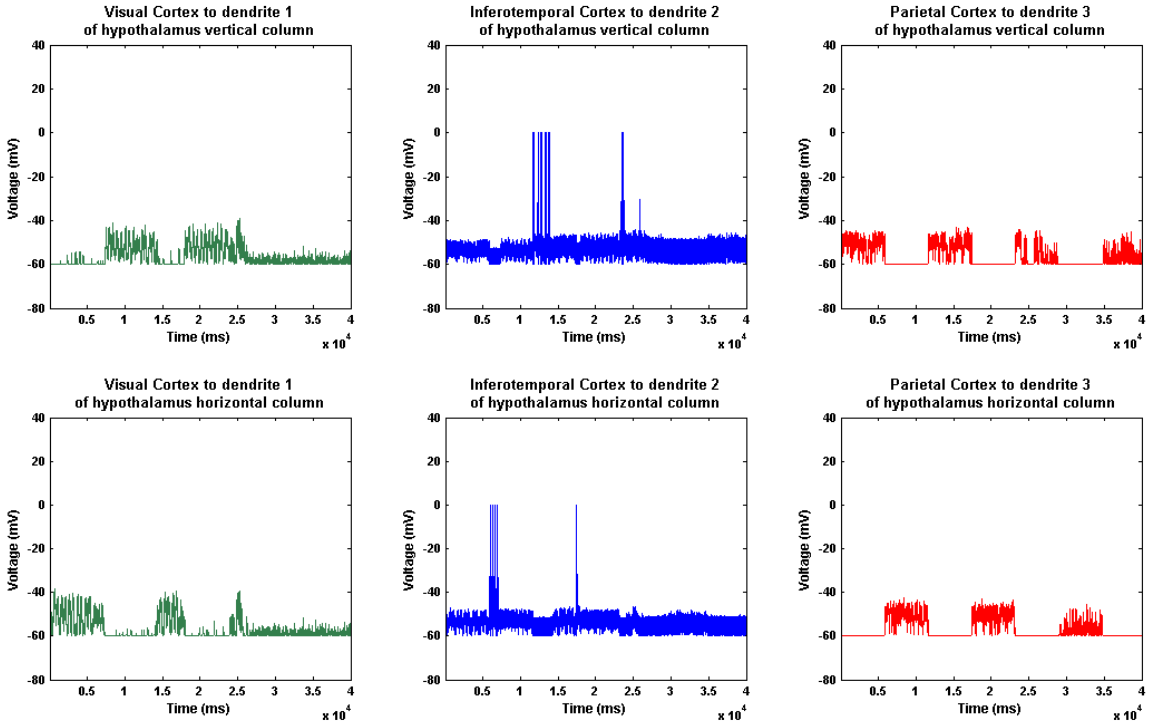

Figure 5.27 Spiking patterns observed within the individual dendrites of the hypothalamus during the discordant motion

5.3. Gabor Screenshots

Figure 5.28 shows the camera view of a human performing the horizontal motion. Figure 5.29 shows the vertical edges of a rod during the horizontal motion. This is due to the Gabor processing of the sequence of frames captured by the camera. Figure 5.30 shows the GUI of the Gabor configuration tool. The purpose of this tool is to specify configuration parameters for either a single or multiple Gabor filters and the NCS communication parameters. The GUI contains a window with a black square overlapping at the center of it that displays the results of the Gabor processing of images as observed in Figure 5.29. A smaller square at the top left corner of the window shows the orientation of the Gabor filter.

Figure 5.28 Camera view of the human motion

Figure 5.29 Vertical edges of a rod detected by the Gabor filter during the human motion

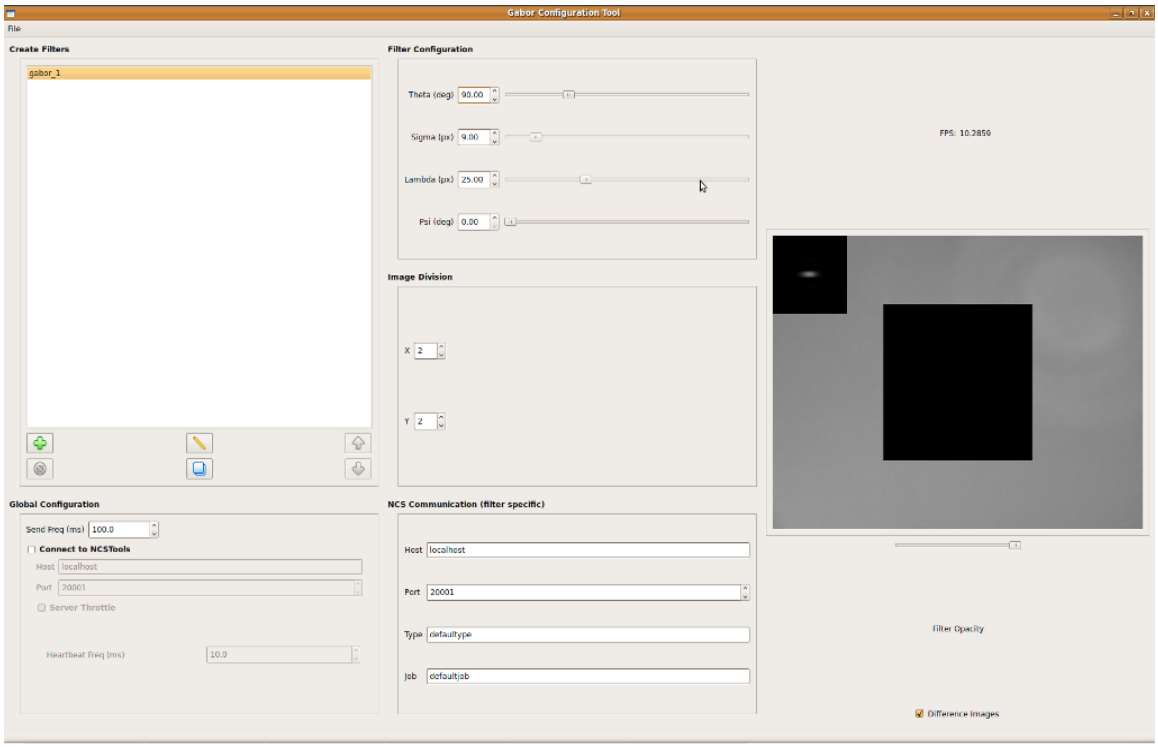

Figure 5.30 Gabor configuration tool used to specify the Gabor filter and NCS communication parameters

5.4. Demonstration of the Instinctual Trust the Intent Scenario

Figure 5.31 shows both the concordant and discordant motions performed by two different people. The top portion of the figure shows a person (me) following the movements of the robot and reaching for an object at a later stage. The robot preemptively hands over the object to the person, since it establishes trust with him. In the bottom portion of the figure, a different person (my colleague, Laurence) performs movements opposite to that of the robot and thus the robot retracts the object towards itself, since it doesn't trust the person. In order to confirm that similar results are observed, the scenario was also run by reversing the roles of the subjects in the experiment, i.e. I performed the discordant motion and Laurence performed the concordant motion.

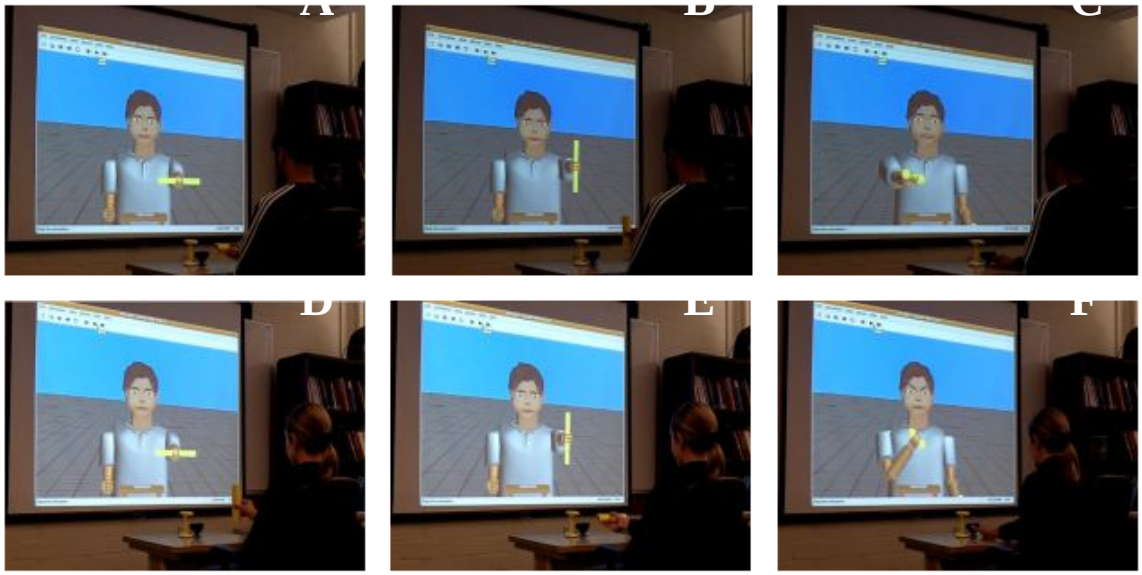

Figure 5.31 Demonstration of the ITI scenario using the VNR loop

Comparison of the Simulation Times

In this study, experiments were performed with and without the RAIN network in the amygdala in order to compare the simulation times. The experiment with the RAIN network active resulted in more simulation time as compared to the experiment without the RAIN network. For the experiment without the RAIN network, a constant monotonic stimulus is injected into the amygdala for the whole simulation period. Table 5.1 shows the amount of time consumed by both the simulations and it can be seen that the experiment with the RAIN network active is not in real-time due to the limitations in the hardware.

Table 5.1 Comparison of the simulation times with and without the RAIN network

	With RAIN	**Without RAIN**
Time (s)	28 – 33	1 – 3

Chapter 6: Conclusions and Future Work

6.1. Conclusions

In this thesis, the findings resulted in the successful modeling of three unique biological aspects of a mammalian brain related to the establishment of trust with an interacting human partner, firing patterns in the hypothalamus due to integrated dendrite potentials, and the introduction of RAIN activity in the amygdala. The research and development presented in this thesis focused on modeling the different regions of a mammalian brain, developing the robotic interface for the ITI scenario, demonstrating the VNR loop as part of the experimental setup, and introducing the triple apical dendrite model within the hypothalamus and the RAIN activity in the amygdala to make the model biologically realistic.

The objective of establishing trust between a VHNR and a human has been achieved. In this process, dendritic release of OT into the hypothalamus [22, 49, 57, 69] is strengthened by reinforcement learning [42] during the concordant action. This in turn causes inhibition of the amygdala RAIN activity thereby suppressing amygdala inhibition of the cortical decision-making circuits. Thus, the trust levels of the VHNR boost up; otherwise, there is no trust being established since the default RAIN activity present in the amygdala suppresses cortical decision-making circuits. A biologically realistic neural circuitry and functioning of the hypothalamic OT, amygdala, and cortical columns present in a mammalian brain were modeled.

The hypothalamic OT cell model has been developed as a realistic four compartment triple apical dendrite model where each dendrite receives stimulus from one of the three cortical columns: visual, partietal, and inferotemporal cortices. The three dendrites integrate and fire the hypothalamus causing a substantial rise in the activity within the hypothalamus. This results in the strengthening of a synaptic USE value of the synapse connecting from the inferotemporal cortex to one of the dendrites of the hypothalamus thereby establishing trust with an interacting human partner.

A self-sustaining RAIN network was introduced in the amygdala to maintain a background activity as observed in a mammalian brain [55]. In the present neuromorphic

brain model, the RAIN network is turned off completely after sufficient learning to trust a person has occurred.

In the work presented in this thesis, the neural circuitry of the hypothalamic OT, amygdala, and cortical columns was successfully implemented on a VHNR to make it trust/distrust its interacting human partner by recognizing his or her intent. Our findings supported the experimental results of Paukner *et al.* (2009) [62] who performed biological experiments on capuchin monkeys and concluded that these monkeys display affiliation towards humans who imitate them. In our model, the VHNR establishes trust with an interacting human partner who imitates it. The VHNR makes a decision about which motor action to perform based on the visual stimulus it receives from the camera. Thus, the visual stimulus plays a prominent role for a neuromorphic brain to make an intelligent decision [72]. In this study, the Gabor processing of images provides the visual stimuli.

The goal of the Brain Computation Lab is not only to develop the brain models but also to emphasize the importance of social robotics. The robotics software package provides a platform to test the brain models. In addition, the integration of the robot simulator, NCS, NCSTools, and camera was a challenge since effective and efficient communication between all these entities is essential to the successful implementation of the experiment.

From this study, it can be concluded that profound knowledge of the hypothalamic OT and amygdala is essential in simulating complex neuromorphic brain models of social cognition that involve the short-term memory [28, 66], trustworthiness [21, 50, 82], and suppression of fear [47, 64]. The transient activation of neural circuitry in the amygdala results in a persistent background activity known as the RAIN network, which could lead to modeling a biologically realistic neuromorphic brain.

6.2. Future Work

The major limitation of this model is that the VNR loop is not running in real-time because of insufficient processing power to handle the RAIN network and the forward and reverse conductances between soma and dendrites in the hypothalamus (these conductances cause spiking in the dendrites connecting to the inferotemporal

cortex). We investigated this situation by shutting down the RAIN network in amygdala and injecting a monotonic stimulus which proved that without the RAIN network the VNR loop runs in perfect real-time. Future work will focus on enhancing the VNR loop such that it will run closer to real time. The instinctual-trust-the-intent model is believed to provide a basis to build complex neuromorphic brain architectures related to memory, trustworthiness, and social phobia, and implement them on virtual and real robots in order to develop intelligent social robots using the VNR loop. For this to become a reality, the present hardware could be replaced with a cluster of higher performance GPUs. The main advantage is that complex brain models containing millions of neurons and quadrillions of synapses can be modeled with the simulations still running in near real-time.

There are only relatively few cells, 1900, being used in the current model. Thus, for more accurate results, the goal is to increase the number of cells in each of the cortical columns from 10 to 100. Moreover, during the concordant motion the RAIN activity present in the amygdala suppresses the activity of the parietal trust column completely after sufficient learning has occurred. But, biologically speaking, while the activity might slide dramatically, it would not cease completely. Hence, as a further enhancement, the aim is to incorporate this biological aspect in the current model.

Furthermore, gaining additional insights into the functioning of the OT could benefit people suffering from autism since it is thought that the OT can ameliorate autism disorders [17, 40]. For example, OT infused into a person suffering from social phobia serves as an inhibitory agent on the amygdala thereby releasing his or her fears, which in turn is a cause to social bonding. This can also help in understanding the reason for social bonding and group living in humans and primate species, which are the key factors for developing multi-agent systems that need to coordinate in order to accomplish specific tasks.

The work presented here contains only the visual stimulus being sent to the NCS. In order to develop humanlike intelligent social robots the auditory stimuli also play a prominent role. Future versions of brain models plan to incorporate the auditory stimuli, which can be sent to the NCS from a microphone. These stimuli can be used as an

emotional reward (positive) or as no reward (negative) to the robot on accomplishing its tasks.

The neuromorphic brain models developed so far deal with simple robot manipulations. Models for robot navigation should be developed wherein a robot should make intelligent decisions while navigating in a complex environment containing obstacles. Finally, the current model has been implemented on a virtual robot and it needs to be tested on a real robot to check the accuracy of the model and the speed of the system.

References

[1] *Action Potential*. [last accessed on September 6th, 2010]; Available at: http://upload.wikimedia.org/wikipedia/commons/c/cc/Action_potential_vert.png.

[2] *Brainstem*. [last accessed on September 6th, 2010]; Available at: http://www.steadyhealth.com/articles/Brainstem_lesions_a282.html.

[3] *Emotions and Learning*. [last accessed on September 6th, 2010]; Available at: http://theelearningcoach.com/learning/emotions-and-learning-part-i.

[4] *Human Cerebral Cortex*. [last accessed on September 6th, 2010]; Available at: http://www.nicertutor.com/class/bio1903/Locked/media/ch48/cerebral.html.

[5] *Interactions of Synapses*. [last accessed on September 6th, 2010]; Available at: http://aids.hallym.ac.kr/d/kns/tutor/ch3-5m.html.

[6] *Lobes of the Brain*. [last accessed on September 6th, 2010]; Available at: http://en.wikipedia.org/wiki/Frontal_lobe.

[7] *NCS User Documentation*. [last accessed on September 6th, 2010]; Available at: http://brain.cs.unr.edu/ncsDocs/ncsUser/TOC.html.

[8] *Neural Control Mechanisms*. [last accessed on September 6th, 2010]; Available at: http://www.biology-online.org/9/7_neural_control_mechanisms.htm.

[9] *The Neuroanatomy of Mind*. [last accessed on September 6th, 2010]; Available at: http://brainmind.com/BrainLecture1.html.

[10] *A Neuron*. [last accessed on September 6th, 2010]; Available at: http://www.doktertomi.com/2009/04/02/contemplating-thought.

[11] *Oxytocin for Shyness*. [last accessed on September 6th, 2010]; Available at: http://scienceblogs.com/corpuscallosum/2007/07/oxytocin_for_shyness_1.php.

[12] *A Synapse*. [last accessed on September 6th, 2010]; Available at: http://webspace.ship.edu/cgboer/synapse.gif.

[13] *Tutorial on Gabor Filters*. [last accessed on September 6th, 2010]; Available at: http://mplab.ucsd.edu/tutorials/gabor.pdf.

[14] *Types of Synapses*. [last accessed on September 6th, 2010]; Available at: http://faculty.washington.edu/chudler/synapse.html.

[15] *Urbi*. [last accessed on September 6th, 2010]; Available at: http://www.gostai.com.

[16] *Webots*. [last accessed on September 6th, 2010]; Available at: http://www.cyberbotics.com.

[17] Andari, E., Duhamel, J. R., Zalla, T., Herbrecht, E., Leboyer, M., and Sirigu, A., "Promoting Social Behavior with Oxytocin in High-Functioning Autism Spectrum Disorders," *Proceedings of the National Academy of Sciences of the United States of America,* vol. 107, pp. 4389-4394, 2010.

[18] Andersonhunt, M., and Dennerstein, L., "Oxytocin and Female Sexuality," *Gynecologic and Obstetric Investigation,* vol. 40, pp. 217-221, 1995.

[19] Bale, T. L., Davis, A. M., Auger, A. P., Dorsa, D. M., and McCarthy, M. M., "CNS Region-Specific Oxytocin Receptor Expression: Importance in Regulation of Anxiety and Sex Behavior," *Journal of Neuroscience,* vol. 21, pp. 2546-2552, 2001.

[20] Barinaga, M., "How Scary Things Get That Way," *Science,* vol. 258, pp. 887-888, 1992.

[21] Baumgartner, T., Heinrichs, M., Vonlanthen, A., Fischbacher, U., and Fehr, E., "Oxytocin Shapes the Neural Circuitry of Trust and Trust Adaptation in Humans," *Neuron,* vol. 58, pp. 639-650, 2008.

[22] Bergquist, F., and Ludwig, M., "Dendritic Transmitter Release: A Comparison of Two Model Systems," *Journal of Neuroendocrinology,* vol. 20, pp. 677-686, 2008.

[23] Bray, L. C. J., Quoy, M., Harris, F. C., and Goodman, P. H., “A Circuit-level Model of Hippocampal Place Field Dynamics Modulated by Entorhinal Grid and Suppression-generating Cells,” *Frontiers in Neural Circuits,* vol. 4, pp. 1-12, 2010.

[24] Brette, R., Rudolph, M., Carnevale, T., Hines, M., Beeman, D., Bower, J. M., Diesmann, M., Morrison, A., Goodman, P. H., Harris, F. C., Zirpe, M., Natschlager, T., Pecevski, D., Ermentrout, B., Djurfeldt, M., Lansner, A., Rochel, O., Vieville, T., Muller, E., Davison, A. P., El Boustani, S., and Destexhe, A., "Simulation of Networks of Spiking Neurons: A Review of Tools and Strategies," *Journal of Computational Neuroscience,* vol. 23, pp. 349-398, 2007.

[25] Carter, C. S., "Developmental Consequences of Oxytocin," *Physiology & Behavior*, vol. 79, pp. 383-397, 2003.

[26] Cavusoglu, M. C., Williams, W., Tendick, F., and Sastry, S. S., "Robotics for Telesurgery: Second Generation Berkeley / UCSF Laparoscopic Telesurgical Workstation and Looking Towards the Future Applications," in *Proceedings of the 39th Allerton Conference on Communication, Control and Computing*, pp. 22-29, 2001.

[27] Choleris, E., Little, S. R., Mong, J. A., Puram, S. V., Langer, R., and Pfaff, D. W., "Microparticle-Based Delivery of Oxytocin Receptor Antisense DNA in the Medial Amygdala Blocks Social Recognition in Female Mice," *Proceedings of the National Academy of Sciences of the United States of America*, vol. 104, pp. 4670-4675, 2007.

[28] Domes, G., Heinrichs, M., Michel, A., Berger, C., and Herpertz, S. C., "Oxytocin Improves 'Mind Reading' in Humans," *Biological Psychiatry*, vol. 61, pp. 731-733, 2007.

[29] Drachman, D. A., "Do We Have Brain to Spare?," *Neurology*, vol. 64, pp. 2004-2005, 2005.

[30] Duncan, J., and Owen, A. M., "Common Regions of the Human Frontal Lobe Recruited by Diverse Cognitive Demands," *Trends in Neurosciences*, vol. 23, pp. 475-483, 2000.

[31] Ebner, K., Bosch, O. J., Kromer, S. A., Singewald, N., and Neumann, I. D., "Release of Oxytocin in the Rat Central Amygdala Modulates Stress-Coping Behavior and the Release of Excitatory Amino Acids," *Neuropsychopharmacology*, vol. 30, pp. 223-230, 2005.

[32] Ferguson, J. N., Young, L. J., and Insel, T. R., "The Neuroendocrine Basis of Social Recognition," *Frontiers in Neuroendocrinology*, vol. 23, pp. 200-224, 2002.

[33] Frye, J., "Parallel Optimization of a Neocortical Simulation Program," [Master's Thesis], University of Nevada, Reno, 2003.

[34] Frye, J., King, J. G., Wilson, J. C., and Harris Jr., F. C., "QQ: Nanoscale Timing and Profiling," in *Proceedings of the 19th IEEE International Parallel and Distributed Processing Symposium*, 2005.

[35] Gray, J. R., Braver, T. S., and Raichle, M. E., "Integration of Emotion and Cognition in the Lateral Prefrontal Cortex," *Proceedings of the National Academy of Sciences of the United States of America*, vol. 99, pp. 4115-4120, 2002.

[36] Gupta, A., Wang, Y., and Markram, H., "Organizing Principles for a Diversity of GABAergic Interneurons and Synapses in the Neocortex," *Science*, vol. 287, pp. 273-278, 2000.

[37] Hairong, F., "Application Study of Fire-Fighting Robot for Railway Tunnel Fire," in *Proceedings of the 2004 International Symposium on Safety Science and Technology*, pp. 1627-1631, 2004.

[38] Hasselmo, M. E., "Methods in Neuronal Modeling - from Ions to Networks (2nd Ed)," *Science*, vol. 282, pp. 1055-1055, 1998.

[39] Heinrichs, M., von Dawans, B., and Domes, G., "Oxytocin, Vasopressin, and Human Social Behavior," *Frontiers in Neuroendocrinology*, vol. 30, pp. 548-557, 2009.

[40] Hollander, E., Novotny, S., Hanratty, M., Yaffe, R., DeCaria, C. M., Aronowitz, B. R., and Mosovich, S., "Oxytocin Infusion Reduces Repetitive Behaviors in Adults with Autistic and Asperger's Disorders," *Neuropsychopharmacology*, vol. 28, pp. 193-198, 2003.

[41] Huber, D., Veinante, P., and Stoop, R., "Vasopressin and Oxytocin Excite Distinct Neuronal Populations in the Central Amygdala," *Science*, vol. 308, pp. 245-248, 2005.

[42] Hurlemann, R., Patin, A., Onur, O. A., Cohen, M. X., Baumgartner, T., Metzler, S., Dziobek, I., Gallinat, J., Wagner, M., Maier, W., and Kendrick, K. M., "Oxytocin Enhances Amygdala-Dependent, Socially Reinforced Learning and Emotional Empathy in Humans," *Journal of Neuroscience*, vol. 30, pp. 4999-5007, 2010.

[43] Ijaz, A., and Aleem, M., "Exogenous Administration of Oxytocin and Its Residual Effects," *Pakistan Veterinary Journal*, vol. 26, pp. 99-100, 2006.

[44] Johansson, C., and Lansner, A., "Towards Cortex Sized Artificial Neural Systems," *Neural Networks*, vol. 20, pp. 48-61, 2007.

[45] Kelley, R., "Mind Reading for Social Robots: Stochastic Models of Intent Recognition," [Master's Thesis], University of Nevada, Reno, 2009.

[46] King, J. G., "Brain Communication Server: A Dynamic Data Transferal System for a Parallel Brain Simulator," [Master's Thesis], University of Nevada, Reno, 2005.

[47] Kirsch, P., Esslinger, C., Chen, Q., Mier, D., Lis, S., Siddhanti, S., Gruppe, H., Mattay, V. S., Gallhofer, B., and Meyer-Lindenberg, A., "Oxytocin Modulates Neural Circuitry for Social Cognition and Fear in Humans," *Journal of Neuroscience,* vol. 25, pp. 11489-11493, 2005.

[48] Koch, C., "Biophysics of Computation: Information Processing in Single Neurons," New York, NY: Oxford University Press, 1999.

[49] Komendantov, A. O., Trayanova, N. A., and Tasker, J. G., "Somato-Dendritic Mechanisms Underlying the Electrophysiological Properties of Hypothalamic Magnocellular Neuroendocrine Cells: A Multicompartmental Model Study," *Journal of Computational Neuroscience,* vol. 23, pp. 143-168, 2007.

[50] Kosfeld, M., Heinrichs, M., Zak, P. J., Fischbacher, U., and Fehr, E., "Oxytocin Increases Trust in Humans," *Nature,* vol. 435, pp. 673-676, 2005.

[51] Lim, M. M., and Young, L. J., "Neuropeptidergic Regulation of Affiliative Behavior and Social Bonding in Animals," *Hormones and Behavior*, vol. 50, pp. 506-517, 2006.

[52] Ludwig, M., and Leng, G., "Dendritic Peptide Release and Peptide-Dependent Behaviours," *Nature Reviews Neuroscience,* vol. 7, pp. 126-136, 2006.

[53] Maciokas, J. B., "Towards an Understanding of the Synergistic Properties of Cortical Processing: A Neuronal Computational Modeling Approach," [PhD Dissertation], University of Nevada, Reno, 2003.

[54] Modi, K. P., "An Application of Human Robot Interaction: Development of a Pingpong Playing Robotic Arm," in *Proceedings of the IEEE International Conference on Systems, Man and Cybernetics,* pp. 1831-1836, 2005.

[55] Mormann, F., Kornblith, S., Quiroga, R. Q., Kraskov, A., Cerf, M., Fried, I., and Koch, C., "Latency and Selectivity of Single Neurons Indicate Hierarchical Processing in the Human Medial Temporal Lobe," *Journal of Neuroscience,* vol. 28, pp. 8865-8872, 2008.

[56] Mountcastle, V. B., "The Columnar Organization of the Neocortex," *Brain,* vol. 120, pp. 701-722, 1997.

[57] Neumann, I. D., "Stimuli and Consequences of Dendritic Release of Oxytocin within the Brain," *Biochemical Society Transactions,* vol. 35, pp. 1252-1257, 2007.

[58] Nguyen, H. G., "Robotics for Law Enforcement: Applications Beyond Explosive Ordnance Disposal," in *Proceedings of SPIE - The International Society for Optical Engineering*, pp. 433-454, 2001.

[59] Ohman, A., "The Role of the Amygdala in Human Fear: Automatic Detection of Threat," *Psychoneuroendocrinology,* vol. 30, pp. 953-958, 2005.

[60] Olshausen, B. A., and Field, D. J., "Emergence of Simple-Cell Receptive Field Properties by Learning a Sparse Code for Natural Images," *Nature,* vol. 381, pp. 607-609, 1996.

[61] Parker, K. J., Buckmaster, C. L., Schatzberg, A. F., and Lyons, D. M., "Intranasal Oxytocin Administration Attenuates the Acth Stress Response in Monkeys," *Psychoneuroendocrinology,* vol. 30, pp. 924-929, 2005.

[62] Paukner, A., Suomi, S. J., Visalberghi, E., and Ferrari, P. F., "Capuchin Monkeys Display Affiliation toward Humans Who Imitate Them," *Science,* vol. 325, pp. 880-883, 2009.

[63] Peng, Q., "Brainstem: A Neocortical Simulator Interface for Robotic Studies," [Master's Thesis], University of Nevada, Reno, 2006.

[64] Petrovic, P., Kalisch, R., Singer, T., and Dolan, R. J., "Oxytocin Attenuates Affective Evaluations of Conditioned Faces and Amygdala Activity," *Journal of Neuroscience,* vol. 28, pp. 6607-6615, 2008.

[65] Purves, D., Augustine, G. J., Fitzpatrick, D., Hall, W. C., LaMantia, A. S., McNamara, J. O., and Williams, S. M., "Neuroscience", Sunderland, MA: Sinauer Associates, Inc., 2004.

[66] Rimmele, U., Hediger, K., Heinrichs, M., and Klaver, P., "Oxytocin Makes a Face in Memory Familiar," *Journal of Neuroscience,* vol. 29, pp. 38-42, 2009.

[67] Ripplinger, M. C., Wilson, C. J., King, J. G., Frye, J., Drewes, R., Harris, F. C., and Goodman, P. H., "Computational Model of Interacting Brain Networks," *Journal of Investigative Medicine,* vol. 52, pp. S155-S155, 2004.

[68] Ross, H. E., and Young, L. J., "Oxytocin and the Neural Mechanisms Regulating Social Cognition and Affiliative Behavior," *Frontiers in Neuroendocrinology,* vol. 30, pp. 534-547, 2009.

[69] Sabatier, N., Rowe, I., and Leng, G., "Central Release of Oxytocin and the Ventromedial Hypothalamus," *Biochemical Society Transactions,* vol. 35, pp. 1247-1251, 2007.

[70] Damasio, A. R., "The Scientific American Book of the Brain," Guilford, CT: The Lyons Press, 1999.

[71] Tahboub, K. A., "Compliant Human-Robot Cooperation Based on Intention Recognition," in *Proceedings of the 2005 IEEE International Symposium on Intelligent Control,* pp. 1417-1422, 2005.

[72] Tosoni, A., Galati, G., Romani, G. L., and Corbetta, M., "Sensory-Motor Mechanisms in Human Parietal Cortex Underlie Arbitrary Visual Decisions," *Nature Neuroscience,* vol. 11, pp. 1446-1453, 2008.

[73] Tsodyks, M. V., and Markram, H., "The Neural Code between Neocortical Pyramidal Neurons Depends on Neurotransmitter Release Probability," *Proceedings of the National Academy of Sciences of the United States of America,* vol. 94, pp. 5495-5495, 1997.

[74] Tsunoda, K., Yamane, Y., Nishizaki, M., and Tanifuji, M., "Complex Objects Are Represented in Macaque Inferotemporal Cortex by the Combination of Feature Columns," *Nature Neuroscience,* vol. 4, pp. 832-838, 2001.

[75] Uvnas-Moberg, K., "Antistress Pattern Induced by Oxytocin," *News in Physiological Sciences,* vol. 13, pp. 22-26, 1998.

[76] Uvnas-Moberg, K., "Oxytocin May Mediate the Benefits of Positive Social Interaction and Emotions," *Psychoneuroendocrinology,* vol. 23, pp. 819-835, 1998.

[77] van't Wout, M., and Sanfey, A. G., "Friend or Foe: The Effect of Implicit Trustworthiness Judgments in Social Decision-Making," *Cognition,* vol. 108, pp. 796-803, 2008.

[78] Vogels, T. P., and Abbott, L. F., "Signal Propagation and Logic Gating in Networks of Integrate-and-Fire Neurons," *Journal of Neuroscience,* vol. 25, pp. 10786-10795, 2005.

[79] Whalen, P. J., Kagan, J., Cook, R. G., Davis, F. C., Kim, H., Polis, S., McLaren, D. G., Somerville, L. H., McLean, A. A., Maxwell, J. S., and Johnstone, T., "Human Amygdala Responsivity to Masked Fearful Eye Whites," *Science*, vol. 306, pp. 2061-2061, 2004.

[80] Wilson, E. C., "Parallel Implementation of a Large-Scale Biologically Realistic Parallel Neocortical-Neural Network Simulator," [Master's Thesis], University of Nevada, Reno, 2001.

[81] Young, L. J., and Wang, Z. X., "The Neurobiology of Pair Bonding," *Nature Neuroscience*, vol. 7, pp. 1048-1054, 2004.

[82] Zak, P. J., Kurzban, R., and Matzner, W. T., "Oxytocin Is Associated with Human Trustworthiness," *Hormones and Behavior*, vol. 48, pp. 522-527, 2005.

[83] Zirpe, M. A., "Rain and NCS5 Benchmarks," [Master's Thesis], University of Nevada, Reno, 2007.